PARAMETRIC INSTABILITY OF A PERIODICALLY SUPPORTED PIPE CONVEYING FLUID

by

SUNIL B. KULKARNI

NUCLEAR ENGINEERING & TECHNOLOGY PROGRAMME

INDIAN INSTITUTE OF TECHNOLOGY KANPUR

SEPTEMBER, 1981

PARAMETRIC INSTABILITY OF A PERIODICALLY SUPPORTED PIPE CONVEYING FLUID

A Thesis Submitted
in Partial Fulfilment of the Requirements
for the Degree of

MASTER OF TECHNOLOGY

by

SUNIL B. KULKARNI

to the

NUCLEAR ENGINEERING & TECHNOLOGY PROGRAMME
INDIAN INSTITUTE OF TECHNOLOGY KANPUR
SEPTEMBER, 1981

16.9.81

CERTIFICATE

This is to certify that the thesis entitled "PARAMETRIC INSTABILITY OF A PERIODICALLY SUPPORTED PIPE CONVEYING FLUID" by Sunil B. Kulkarni is a record of work carried out under our supervision and has not been submitted elsewhere for a degree.

A.K. Mallik
Assistant Professor
Department of Mechanical Engineering,
Indian Institute of Technology, Kanpur.

K. Sri Ram
Professor and Head
Nuclear Engineering and Technology Programme,
Indian Institute of Technology, Kanpur.

September, 1981

To

My patient

mother

Acknowledgement

I wish to sincerely acknowledge my gratitude to my teachers Dr. A.K. Mallik and Dr. K. Sri Ram in connection with this work.

I am grateful to Dr. A.K. Mallik for having taught me all about vibrations in his inimitable style of teaching and furthermore I am indebted to him for having suggested the outline of this work and his earnest guidance.

To Dr. K. Sri Ram I owe my gratitude for having cultivated in me an interest in Nuclear Engineering and for his constant assistance during the progress of this thesis.

Indeed it has been my good fortune to have had such teachers as Dr. A.K. Mallik and Dr. K. Sri Ram who fulfil in a more than complete manner, the student's expectations of his masters.

I am also grateful to my tribe of friends for having patiently given ear to my frequent if not welcome monologues on this work.

Lastly, I wish to acknowledge the contribution of Shri J.P. Gupta, Shri R.S. Tripathi and Shri Verma for their labours in the preparation of this thesis.

Sunil B. Kulkarni

CONTENTS

LIST OF FIGURES

LIST OF TABLES

SYNOPSIS

PARAMETRIC INSTABILITY OF A PERIODICALLY SUPPORTED PIPE CONVEYING FLUID

This thesis is a study of the parametric instabilities of a periodically supported pipe conveying a pulsatile flow. The velocity of the fluid is considered to have a harmonic fluctuation over and above the mean constant value. This work demonstrates that the method of propagation constants can be used efficiently for analysis of periodic structures vuluerable to flow induced parametric vibrations. In the same range of frequencies the number of instability zones increases with larger number of spans. The power of the method lies in rendering the computational effort independent of the number of spans. In addition, zones of instabilities associated with all the modes are determined simultaneously. Bolotin's method has been used to investigate the bounds for the principal primary regions of instability. Single span pipe receptances used in the analysis have been obtained without taking recourse to mode shape approximation. The coupling effect due to fluid inertia has been taken into account systematically. It is shown that the instability zones can be controlled effectively by the use of damped dynamic absorbers.

CHAPTER - I

INTRODUCTION

1.1 Introduction

Pipelines conveying fluids at high velocities are encountered in various fields of engineering. To name a few, such pipelines exist in the coolant channels of nuclear reactors, high pressure boilers, process industries and fuel lines of aircrafts and missiles. Due to fluctuations in the fluid speed (generated for example by the fluid driving pump) such systems are vulnerable to parametric instabilities. In severe cases, excessive vibration of the pipelines may even cause fatigue cracks and eventual failure of the pipes.

Failure of the coolant channels in a nuclear reactor has hazardous consequences. In addition to hazard, the high cost of equipment in special applications demands a high degree of reliability in the subsystems. Due to these reasons, a thorough understanding of the stability domains of these pipelines is necessary to ensure proper design.

With increasingly high flow speeds required in engineering applications, considerable amount of research work has been done in recent years, in the field of flow induced vibrations. A variety of instabilities have been

uncovered at high flow speeds that have gone in making this subject a theoretician's delight and a designer's nightmare. A fluid flowing (under suitable conditions) in a flexible pipe is known to induce static buckling (divergence instability), combinational resonances, parametric instabilities, etc., to name a few.

Most of the volume of literature is devoted to the analysis of a single span pipe. In actual practice however, more often we encounter multispanned pipes where analysis becomes increasingly difficult with increasing number of spans.

The present work is a study of the parametric instabilities of a uniform pipe placed on equispaced supports and carrying a pulsatile flow. Multispan pipes display more number of instability zones in comparison to a single span pipe in the same range of frequencies. The method of approach used is one that renders the computational effort independent of the number of spans. In addition, it enables one to obtain the zones of instability, associated with the higher modes of a multispan pipe, without involving any further steps in the analysis. The objective and scope of this thesis is outlined in detail in a later section.

1.2 Review of Previous Work

Since the present work deals with the dynamics of pipes conveying fluids and analysis of periodic structures,

a brief review of the available literature in each of these fields is given in the following sections.

1.2.1 Dynamics of Pipes Conveying Fluids

Interest in the study of dynamics of elastic pipes conveying fluids was reactivated in 1950 by Ashley and Haviland [1], in connection with the vibration problems of Trans Arabian pipelines. It was observed that the effect of the flow is to damp the transverse vibrations and that the flow induced damping (a non viscous effect) decreases the response at higher flow rates. Long [2] pointed the errors in their analysis and showed that damping by internal flow occurs only in a certain range of flow velocities. Housner [3] reported that at sufficiently high flow velocities the pipe may buckle, essentially like a column subjected to axial loading. Gregory and Paidoussis [4] showed for high flow rates oscillatory instabilities are possible and that the dynamical problem is independent of fluid friction. An extensive literature survey in the subsequent developments is presented in reference [5].

Chen [6] studied the problem with the velocity of the flowing fluid having a harmonic fluctuation over and above the mean constant value. He found that both parametric and combinational resonances are possible. He determined the instability regions for a simply supported pipe. The

governing equation was revised by Paidoussis and Issid [7] and the regions of parametric instability for single span pipe with various end conditions were obtained by the Ritz-Galerkin method.

1.2.2 Analysis of Periodic Structures

Wave motion in periodic systems in the field of crystals, electrical circuits, etc. has been studied for nearly 300 years, as pointed out by Brillouin [8] in his classical work. The extension of this method for the analysis of wave motion in engineering structures (consisting of beams, plates, etc.) is a recent phenomenon.

Mead [9] studied the free wave propagation in infinite beams on periodic supports using the propagation constants approach. Based on the wave approach Sengupta [10] developed a graphical method, to determine the natural frequencies of a finite periodic beam.

Singh and Mallik [11] studied the wave propagation and vibration response of a periodically supported pipe conveying fluid. They showed that due to the presence of the coriolis term in the equation of motion, classical normal modes (standing modes) do not exist. Conditions for both divergence instability (buckling) and oscillatory instability (resonance) were obtained by the wave approach.

A succeeding paper by the same authors [12] was devoted to obtaining the instability regions associated with parametric excitation of the same system. In this work it was shown that all the instability zones are insensitive to the fluid mass ratio parameter so that the graphical approach is valid for determination of the instability regions. The analysis was based on the governing equation as obtained by Chen [6]. Based on the assumptions in [12], the effect of a dynamic absorber on the instability zones of a single span pipe was reported by Singh and Mallik [13]. Mallik and Narayanan [14] extended the analysis for a periodically supported pipe with a vibration absorber in each span. It was shown that the instability regions can be controlled effectively by damped absorbers.

1.3 Objective and Scope of the Present Work

In all these works on parametric excitation of periodically supported pipes, it is observed that in the initial steps of the wave analysis, certain assumptions are incorporated that implicitly ignore the coupling terms. The results in these analyses are consequently insensitive to the change of the degree of coupling (that is given by the fluid mass ratio parameter.). Though these assumptions, simplify the analysis greatly, this thesis bears it out that certain important conclusions reached in these works are

erroneous. It is also remarked that the governing equation used in these works is based on that of references [16] and [15], which have been shown to be incorrect [7].

The present thesis is an attempt to rectify these shortcomings in the previous analyses by a rigorous application of the propagation constants approach. Moreover the correct equation of motion which has non-constant coefficients is used. The coupling effects have been retained at all stages of the analysis, and it is shown under what restricted situations and stages of analysis are the conclusions of the above mentioned references justifiable.

As mentioned before, the computational effort, in the methodology used, is independent of the number of spans. Computations have been undertaken only for the case of one span and two span pipes for the sake of brevity and for comparison with the results of previous works.

As long as the periodicity in the structure is maintained, the method can be used for any type of support conditions. For the sake of simplicity it is assumed in this work that the pipe is placed on line supports (i.e. no axial force and no torsional restraint is produced by the supports). Due to complexity of the governing equation, no mode shape approximations have been resorted to. The transverse displacement has been expressed as a truncated power series of suitable order so as to obtain the desired accuracy.

The effect of attaching a dynamic absorber at the midspan of each bay, is also investigated. It is demonstrated that, by suitably changing the absorber parameters, the instability zones (in excitation parameter/ frequency space) can be effectively controlled. The matter has not been explored beyond this stage since optimisation of the absorber parameters would be a separate topic in itself. The analysis has been restricted only to the determination of the principal primary instability regions.

The present thesis may be broadly divided into three sections :

i) Determination of propagation constants for an infinite periodic pipe.

ii) Determination of the zones of parametric instabilities of a finite periodically supported pipe.

iii) Investigation of the effect of dynamic absorbers on the instability zones of these pipes.

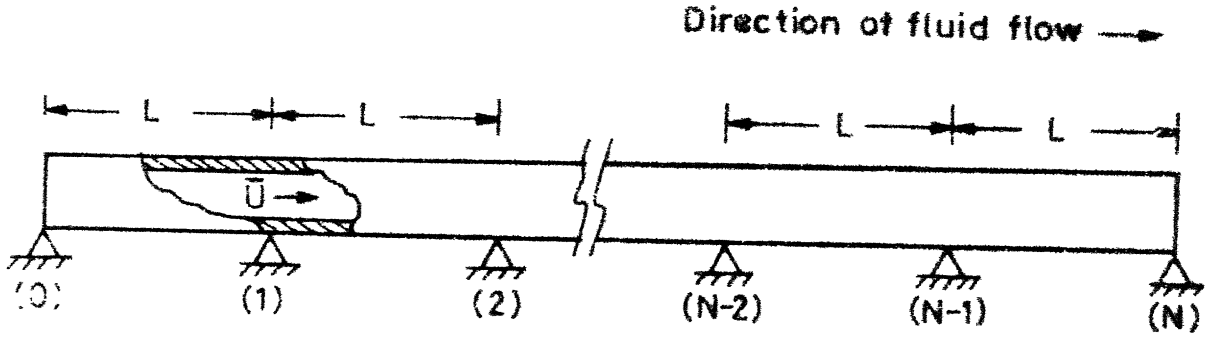

Fig. 2·1 Periodically supported N-span pipe conveying fluid

CHAPTER - II

PARAMETRIC INSTABILITY OF A PERIODICALLY SUPPORTED PIPE CONVEYING FLUID

2.1 Introduction

In this chapter we shall discuss the means of obtaining the instability bounds of a parametrically excited pipe placed on equidistant line supports. For a pipe of N spans we have adopted the convention of naming the supports as 0, 1, 2,..., N as shown in Fig. (2.1). In section 2.2 the governing equation for such a pipe carrying time dependent flow is discussed. We assume the flow to have a harmonic fluctuation over and above a mean velocity. In section 2.3 the governing equation is reduced to a form amenable for further analysis, especially for the determination of regions of instabilities. A periodically supported pipe of infinite number of spans can be considered to be composed of identical members, each of one span length, connected together to the adjacent members in an identical manner. In section 2.4 using this spatial periodicity, a functional relationship of the propagation constants in terms of the single span receptances is obtained, so as to satisfy the intermediate support constraints. Section 2.5 is devoted to develop the equation for obtaining the frequencies bounding the instability zones, by application of the end support constraints for an N-span pipe. In section 2.6 an outline of the method to obtain the

receptances for a single span pipe is presented. A particula case of parameter values for which the analysis is simplified is discussed in section 2.7. Lastly in section 2.8 the discussion of results and computations is undertaken.

2.2 Equations of Motion

The equation for transverse motion of a pipe carryin a time dependent flow, in the absence of external loading is [

$$E^{*} I \frac{\partial^5 \bar{w}}{\partial \bar{x} \partial \tau} + EI \frac{\partial^4 \bar{w}}{\partial \bar{x}^4} + (m_f+m_p) g' \frac{\partial \bar{w}}{\partial \bar{x}} +$$

$$[m_f \cdot \bar{U}^2 - \bar{T} + pA (1 - 2 vf) - ((m_f+m_p) g' - m_f \frac{\partial \bar{U}}{\partial \tau})(L-\bar{x})] \frac{\partial^2}{\partial \bar{x}}$$

$$+ 2 m_f \bar{U} \frac{\partial^2 \bar{w}}{\partial \bar{x} \partial \tau} + c \frac{\partial \bar{w}}{\partial \tau} + (m_f+m_p) \frac{\partial^2 \bar{w}}{\partial \tau^2} = 0,$$

$$0 \leq \bar{x} \leq L , \quad \ldots(2.01)$$

where,

τ is the independent time variable,

$\bar{x}$ is the independent length coordinate along the pipe axis,

L is the unsupported pipe length between two adjacent supports,

$\bar{w}$ is the transverse pipe displacement and is a function of both $\bar{x}$ and τ,

I is the cross sectional moment of inertia, of the pipe

E^* is the viscoelastic coefficient of internal dissipation,

E is the elastic modulus,

m_f is the mass of the fluid per unit length,

m_p is the mass of the pipe per unit length,

g' is the axial component of the gravitational acceleration,

$\bar{U}$ is the time dependent bulk velocity of the fluid,

$\bar{T}$ is the externally applied tension,

p is the fluid pressure,

A is the internal pipe cross sectional area,

v is Poissons ratio,

$f=0$ with no axial constraint at the supports,

$f=1$ with axial constraint at the supports, and

c is the coefficient of viscous damping applicable to transverse motion of the pipe.

Equation (2.01) was derived with the following assumptions :

(1) The amplitude of transverse oscillations is small with respect to the length of the vibrating pipe.

(2) The fluid is inviscid and incompressible and has a plug flow profile.

(3) The flow is uninfluenced by the transverse motion of the pipe.

To simplify the analysis we retain only certain terms and make the following additional assumptions :

(1) Low damping in pipe material, implying $E^{*} = 0$.

(2) Pipe is horizontally placed, for which case $g' = 0$.

(3) No axial tension, or $\bar{T} = 0$.

(4) Negligible effect of pressurisation, i.e. $p = 0$.

(5) External viscous damping is very small, or $c = 0$.

With these assumptions, the governing equation (2.01) reduces to,

$$EI \frac{\partial^4 \bar{w}}{\partial \bar{x}^4} + m_f \bar{U}^2 \frac{\partial^2 \bar{w}}{\partial \bar{x}^2} + [m_f(L-\bar{x}) \frac{\partial \bar{U}}{\partial \tau}] \frac{\partial^2 \bar{w}}{\partial \bar{x}^2} + 2m_f \bar{U} \frac{\partial^2 \bar{w}}{\partial \bar{x} \partial \tau}$$

$$+ (m_f + m_p) \frac{\partial^2 \bar{w}}{\partial \tau^2} = 0, \quad 0 \leq \bar{x} \leq L \quad \ldots(2.02)$$

The non-dimensional form of equation (2.02) is,

$$\frac{\partial^4 w}{\partial x^4} + u^2 \frac{\partial^2 w}{\partial x^2} + [\gamma(1-x) \frac{\partial u}{\partial t}] \frac{\partial^2 w}{\partial x^2} + 2\gamma u \frac{\partial^2 w}{\partial x \partial t} + \frac{\partial^2 w}{\partial t^2} = 0,$$

$$0 \leq x \leq 1 \quad \ldots(2.03)$$

where the following non-dimensional parameters are used:

(1) Transverse displacement $w = \bar{w}/L$,

(2) Fluid velocity $u = \bar{U} \left[\frac{L^2 m_f}{EI}\right]^{1/2}$,

(3) Axial coordinate $x = \bar{x}/L$,

(4) Time $t = \tau \left[\frac{EI}{(m_f + m_p)L^4} \right]^{1/2}$,

(5) Fluid mass ratio parameter $\gamma = \left[\frac{m_f}{m_f + m_p} \right]^{1/2}$.

In equation (2.03) the leading term represents the flexural force and the fifth term represents the total inertia force due to transverse motion of the pipe and fluid. The second term arises due to reaction on the pipe by the fluid as it moves in a curved path due to pipe flexure (centrifugal effect). The third term arises due to the time dependent nature of the flow. Also as the pipe is undergoing transverse vibration, at each point the slope of the pipe changes with time (and hence the fluid is forced to rotate at each point) causing a coriolis force to act on the pipe represented by the fourth term. This coriolis term causes coupling between the spatial modes of the pipe, the implications of which, will be evident later. It may be noted that the second term is equivalent to an axial compressive load on the pipe and for a suitably high magnitude of u causes static buckling [11].

In this work, a pulsatile flow has been modelled as a non-zero quiscent flow carrying a harmonic rider which is represented thus,

$$u = u_o (1 + \delta \cos \Omega t) \qquad \ldots(2.04)$$

where u_o is the quiscent fluid velocity and δ is the excitation parameter, and Ω is the non-dimensional frequency given by $\frac{\omega\tau}{t}$ with ω rad/time as the dimensional frequency.

Substituting equation (2.04) in equation (2.03) one gets,

$$\frac{\partial^4 w}{\partial 4} + [u_o^2(1 + \delta\cos \Omega t)^2 - \gamma u_o \delta \Omega(1-x)\sin \Omega t \,] \frac{\partial^2 w}{\partial x^2}$$

$$+ 2\gamma u_o(1+\delta\cos \Omega t) \frac{\partial^2 w}{\partial x \partial t} + \frac{\partial^2 w}{\partial t^2} = 0, \quad 0 \leq x \leq L$$

...(2.05)

The coefficients of various terms in equation (2.05) are time varying and hence the system is said to be parametrically excited. With constant parameters (i.e. coefficients) the system would have had instabilities at certain discrete frequencies. The effect of parametric excitation (due to time dependent velocity in our case) manifests itself by causing the system to have unbounded solutions (instabilities) at certain discretely spaced frequency bands for a given value of the excitation parameter, δ. The unstable regions are normally plotted in the $\Omega - \delta$ space.

2.3 Determination of Regions of Parametric Instabilities

The regions of primary instability of equation (2.05) are bounded by periodic solutions of period 2T where $T = \frac{2\pi}{\Omega}$. Hence, on the boundary, the transverse displacement can be expressed as [16],

$$w(x,t) = \sum_{K=1,3,5,\ldots} \left(X_K(x)\sin\left(\frac{\Omega t}{2}\right) + Y_K(x)\cos\left(\frac{\Omega t}{2}\right)\right) \quad \ldots(2.06)$$

The region of principal primary instability can be obtained quite accurately by truncating the series in equation (2.06) at K = 1 itself [16]. Hence one can write

$$w(x,t) = X(x)\sin\left(\frac{\Omega t}{2}\right) + Y(x)\cos\left(\frac{\Omega t}{2}\right) \quad \ldots(2.07)$$

where, for convenience we dispense off the subscripts on X(x) and Y(x). In this approximation we are neglecting the instability zones arising due to K = 3,5,.... This step is justifiable since the higher instability zones are very narrow and are therefore of negligible interest. Also, by retaining the terms with K > 1 in the equation (2.06) for w(x,t), the principal primary instability zones are progressively modified, but the change whatsoever is small and may be neglected. Substituting equation (2.07) in equation (2.05) and equating coefficients of $\sin\left(\frac{\Omega t}{2}\right)$ and $\cos\left(\frac{\Omega t}{2}\right)$ separately to zero, we get,

$$\frac{d^4X}{dx^4} + u_o^2 \left(1-\delta+\frac{\delta^2}{2}\right) \frac{d^2X}{dx^2} - \frac{1}{4}\Omega^2 X$$

$$- \frac{\gamma u_o \delta \Omega}{2} \left[(1-x) \frac{d^2Y}{dx^2} - \left(1 - \frac{2}{\delta}\right) \frac{dY}{dx}\right] = 0, \quad 0 \leq x \leq 1,$$

...(2.08a)

$$\frac{d^4Y}{dx^4} + u_o^2 \left(1+\delta+\frac{\delta^2}{2}\right) \frac{d^2Y}{dx^2} - \frac{1}{4}\Omega^2 Y$$

$$- \frac{\gamma u_o \delta \Omega}{2} \left[(1-x) \frac{d^2X}{dx^2} - \left(1 + \frac{2}{\delta}\right) \frac{dX}{dx}\right] = 0, \quad 0 \leq x \leq 1,$$

...(2.08b)

These are two fourth order coupled ordinary differential equations with non-constant coefficients. The coupling between the equations of X(x) and Y(x) originates from the terms arising due to unsteady flow velocity and the coriolis acceleration. For $\gamma = 0$, equations (2.08a and b) are decoupled and analysis becomes simpler. This case is discussed in section 2.7.

It is shown in reference [5] that the influence of neglecting the coupling terms (i.e. making the $\gamma = 0$ approximation for the situations in which γ is actually non-zero) does not change the instability zones significantly. However due to some inconsistencies in the analysis presented there and in view of the improved governing equation (2.01) which is different from that used in reference [5], the effect of γ on the stability zones needs fresh investigation. With this aim the coupling terms are retained for further analysis.

For a given set of parameter values the instability bounding frequencies are those at which equation (2.08a and b) are satisfied alongwith the boundary conditions of the pipe. For example in the case of a single span pipe placed on line supports at both ends the relevant boundary conditions at $x = 0$ and $x = 1$ are,

$$w(o,t) = X(o)\sin(\frac{\Omega t}{2}) + Y(o)\cos(\frac{\Omega t}{2}) = 0 \qquad (2.09a)$$

$$w(1,t) = X(1)\sin(\frac{\Omega t}{2}) + Y(1)\cos(\frac{\Omega t}{2}) = 0 \qquad (2.09b)$$

$$\frac{\partial^2 w}{\partial x^2}(o,t) = X''(o)\sin(\frac{\Omega t}{2}) + Y''(o)\cos(\frac{\Omega t}{2}) = 0 \qquad (2.09c)$$

$$\frac{\partial^2 w}{\partial x^2}(1,t) = X''(1)\sin(\frac{\Omega t}{2}) + Y''(1)\cos(\frac{\Omega t}{2}) = 0 \qquad (2.09d)$$

In terms of X and Y equations (2.9a,b,c,d) may be written as

$$X(o) = Y(o) = 0 \qquad (2.09e)$$

$$X''(o) = Y''(o) = 0 \qquad (2.09f)$$

$$X(1) = Y(1) = 0 \qquad (2.09g)$$

$$X''(1) = Y''(1) = 0 \qquad (2.09h)$$

Thus for a single span, the system of equations (2.08a,b) consists of 8 unknowns and 8 boundary conditions (2.09e,f,g,h).

By solving for the eigen values of the coupled equations (2.08a,b) with the appropriate boundary conditions, we obtain the frequencies at which a non-trivial solution exists. These frequencies then corresponds to the bounding frequencies of the instability zones for a single span. Extension of this method (referred to as the direct method) for a pipe consisting of a large number of spans is unweildy as 8 boundary conditions are to be satisfied at every intermediate support over and above satisfying four boundary conditions at each end support. Thus for an N-span pipe, the frequency determinant (zeroes of which gives the eigen values) is of the order 8N x 8N. The direct approach becomes unwieldy due to the appearance of numerous intermediate support conditions, for large number of spans.

However, if an N-span pipe is periodic in nature i.e. consists of identical elements connected together in an identical fashion, then the intermediate conditions between any two elements are identical in nature. In such a case, all the information contained in the many intermediate supports, may be substituted by obtaining a set of propagation constants (to be explained later) by satisfying all the constraints at any one of the intermediate supports. By this approach the computational effort is rendered independent of the number of spans. This method using the concept of propagation constants is outlined in the subsequent section.

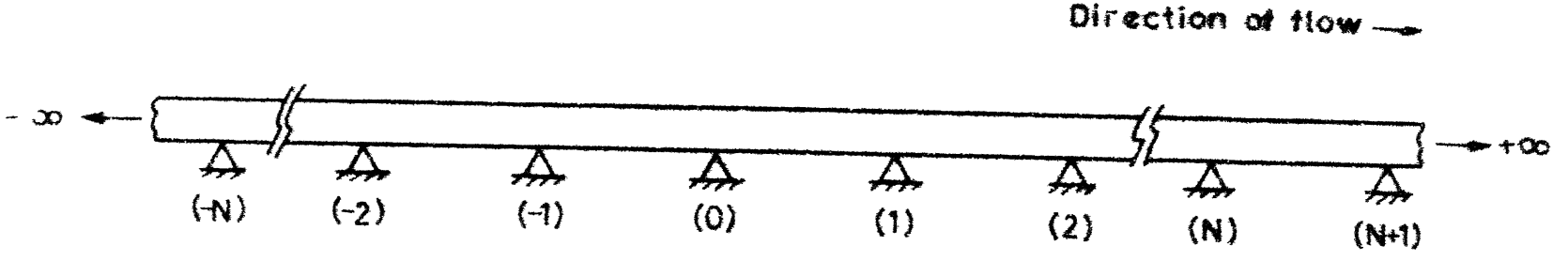

Fig. 2·2 (a) Periodically supported infinite pipe conveying fluid

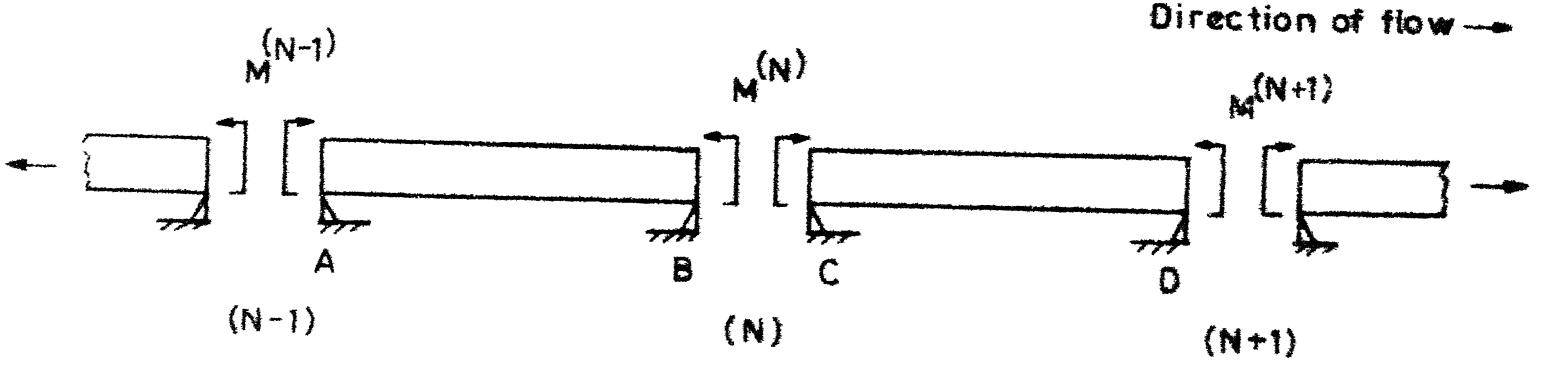

Fig. 2·2 (b) Two adjacent periodic elements of the infinite pipe at the (N) th support

2.4 Determination of Propagation Constants for an Infinite Periodically Supported Pipe

Let us consider a pipe, infinite in extent, placed on equispaced line supports as shown in Fig. (2.2a) and carrying a flow described by equation (2.04). Equations (2.08a, b) then apply to each span of this pipe. We shall satisfy the slope continuity at say the Nth junction in the following manner. Consider the two spans AB and CD, adjacent to the Nth support as shown in Fig. (2.2b). Let M_{N-1} and M_n be the non-dimensionalised moments ($M_N = \bar{M}_N \frac{L}{EI}$, where $\bar{M}_N$ is the dimensional moment) acting on the two ends of the span AB. We have satisfied moment continuity relation at the Nth support by assuming M_N to act on both B and C. Let θ_B and θ_C represent the slope of the pipe at ends B and C respectively. For the system response : w(x,t) given by equation (2.07) we may consider the slope and movement at any location to be similar harmonic time functions of frequency ($\frac{}{2}$). Hence we designate the following coefficients (unknowns): $\theta_{B\,q}$; $\theta_{C\,q}$; $M_q^{(N-1)}$, $M_q^{(N)}$, $M_q^{(N+1)}$; q=x,y such that :

$$\left(\frac{w}{x}\right)_B = \theta_B = \theta_{Bx} \sin\left(\frac{t}{2}\right) + \theta_{By} \qquad \ldots(2.09a)$$

$$\left(\frac{\partial w}{\partial x}\right)_C = \theta_C = \theta_{Cx} \sin\left(\frac{\Omega t}{2}\right) + \theta_{Cy} \cos\left(\frac{\Omega t}{2}\right) \quad \ldots(2.09b)$$

$$M^{(N+1)} = M_x^{(N+1)} \sin\left(\frac{\Omega t}{2}\right) + M_y^{(N)} \cos\left(\frac{\Omega t}{2}\right) \quad \ldots(2.10a)$$

$$M^{(N)} = M_x^{(N)} \sin\left(\frac{\Omega t}{2}\right) + M_y^{(N)} \cos\left(\frac{\Omega t}{2}\right) \quad \ldots(2.10b)$$

$$M^{(N-1)} = M_x^{(N-1)} \sin\left(\frac{\Omega t}{2}\right) + M_y^{(N-1)} \cos\left(\frac{\Omega t}{2}\right) \quad \ldots(2.10c)$$

Using the influence coefficients or receptance method, the slope at B may be expressed as a linear combination of the end moments acting on the span AB. Due to coupling in the governing equation (2.08a,b) a sinusoidally varying end moment in addition to exciting a sinusoidal response also generates a cosine response. To this end we may distinguish the receptances for a single span pipe in two categories.

(1) Direct receptances :

Response at A and B to a unit moment acting at one of the ends which is in phase with the exciting moment.

(2) Cross receptances :

The response at A and B which is out of phase (by $\pm \frac{\pi}{2}$) with the exciting moment acting at either of the two ends.

With this in mind θ_{Bx}, θ_{By} may be expressed, in general, as a linear combination of the four types of moments $M_x^{(N-1)}$, $M_y^{(N-1)}$, $M_x^{(N)}$, $M_y^{(N)}$ acting on pipe element AB, as below :

$$\theta_{Bx} = \beta_{11}^{xx} M_x^{(N)} + \beta_{11}^{xy} M_y^{(N)} + \beta_{10}^{xx} M_x^{(N-1)} + \beta_{10}^{xy} M_y^{(N-1)} \quad \ldots(2.11a)$$

$$\theta_{By} = \beta_{11}^{yx} M_x^{(N)} + \beta_{11}^{yy} M_y^{(N)} + \beta_{10}^{yx} M_x^{(N-1)} + \beta_{10}^{yy} M_y^{(N-1)} \quad \ldots(2.11b)$$

where for example β_{10}^{xy} is defined as the amplitude of the sinusoidally varying slope response at the right end (1) of the span generated by a unit cosinusoidal moment acting on the left end (o) of the span. The remaining receptances are defined and scripted similarly. The direct receptances are identified as β_{ij}^{xx} and β_{ij}^{yy}, $i = 0,1$; $j = 0,1$ and the cross receptances correspond to the type $\beta_{i,j}^{xy}$ and $\beta_{i,j}^{yx}$, $i = 0,1$ and $j = 0,1$. The receptances β's are properties of a single span pipe as governed by equation (2.08a, b) and are functions of the non-dimensional frequency Ω and other system parameters only. The method for computing the receptances is outlined in section 2.7. Since the spans AB and CD have identical physical parameters a similar set of receptances may be used to express θ_{Cx} and θ_{Cy} in terms of the end

moments acting on span CD. Hence

$$\theta_{Cx} = \beta_{00}^{xx} M_x^{(N)} + \beta_{00}^{xy} M_y^{(N)} + \beta_{01}^{xx} M_x^{(N+1)} + \beta_{01}^{xy} M_y^{(N+1)} \quad \ldots(2.12a)$$

$$\theta_{Cy} = \beta_{00}^{yx} M_x^{(N)} + \beta_{00}^{yy} M_y^{(N)} + \beta_{01}^{yx} M_x^{(N+1)} + \beta_{01}^{yy} M_y^{(N+1)} \quad \ldots(2.12b)$$

It is remarked that $\beta_{00}^{xx} \neq \beta_{11}^{xx}$, $\beta_{00}^{yy} \neq \beta_{11}^{yy}$ due to the directional assymmetry imposed by the flow and the consequent appearance of terms depending on u, $\dot{u}$ in the governing equation (2.03). However a restricted sort of equivalence can hold between certain cross receptances and this is discussed later section 2.7.

For the condition of slope continuity $\theta_B = \theta_C$, to be true for all time, the sine and cosine components of the two functions must necessarily be equal. i.e.,

$$\theta_{Bx} = \theta_{Cx} \quad \ldots(2.13a)$$

$$\theta_{By} = \theta_{Cy} \quad \ldots(2.13b)$$

Substituting the expressions for θ_{Bx} and θ_{Cx} from equations (2.11a) and (2.12b) in (2.13a) and subsequently rearranging the terms one obtains

$$\beta_{10}^{xx} M_x^{(N-1)} + (\beta_{11}^{xx} - \beta_{00}^{xx}) M_x^{(N)} - \beta_{01}^{xx} M_x^{(N+1)} = \beta_{01}^{xy} M_y^{(N+1)}$$

$$+ (\beta_{00}^{xy} - \beta_{11}^{xy}) M_y^{(N)} - \beta_{10}^{xy} M_y^{(N-1)} \quad \ldots(2.14a)$$

and similarly from equations (2.11b), (2.12b) and (2.13b) we get,

$$\beta_{10}^{yx} M_x^{(N-1)} + (\beta_{11}^{yx} - \beta_{00}^{yx}) M_x^{(N)} - \beta_{01}^{yx} M_x^{(N+1)} = \beta_{01}^{yy} M_y^{(N+1)}$$

$$+ (\beta_{00}^{yy} - \beta_{11}^{yy}) M_y^{(N)} - \beta_{10}^{yy} M^{(N-1)} \qquad \ldots(2.14b)$$

Due to spatial periodicity [9], a relationship which holds between two quantities (e.g. slope or moment) at one pair of adjacent supports must necessarily also hold true at all other pairs of adjacent supports as well. Thus equations (2.14a) and (2.14b) can be written for any three consecutive supports. Solution of these coupled difference equation may be written in the following form

$$\frac{M_x^{(1)}}{M_x^{(0)}} = \frac{M_x^{(2)}}{M_x^{(1)}} = \ldots\ldots \frac{M_x^{(N)}}{M_x^{(N-1)}} = \frac{M_x^{(N+1)}}{M_x^{(N)}} = \ldots\ldots = e^{+\mu} \qquad \ldots(2.15a)$$

and

$$\frac{M_y^{(1)}}{M_y^{(0)}} = \frac{M_y^{(2)}}{M_y^{(1)}} = \ldots\ldots \frac{M_y^{(N)}}{M_y^{(N-1)}} = \frac{M_y^{(N+1)}}{M_y^{(N)}} = \ldots\ldots = e^{+\mu} \qquad \ldots(2.15b)$$

where μ, is termed as the propagation constant [9]. In general, μ is a complex number where the real part signifies the logarithmic decrement per span and the imaginary component signifies the phase change per span.

Substituting the moments at the (N+1)th and (N-1)th supports in terms of moments at the (N)th support in equation (2.14a,b) we obtain

$$[\beta_{01}^{xx}\cdot(e^{\mu})^2 + (\beta_{00}^{xx} - \beta_{11}^{xx})\cdot(e^{\mu}) - \beta_{10}^{xx}]\, M_x^{(N)}$$

$$+ [\beta_{01}^{xy}\cdot(e^{\mu})^2+(\beta_{00}^{xy} - \beta_{11}^{xy})(e^{\mu})-\beta_{10}^{xy}]\, M_y^{(N)} = 0$$

...(2.16a)

$$[\beta_{01}^{yx}\cdot(e^{\mu})^2 + (\beta_{00}^{yx} - \beta_{11}^{yx})\cdot(e^{\mu}) - \beta_{10}^{yx}]\, M_x^{(N)}$$

$$+ [\beta_{01}^{yy}\cdot(e^{\mu})^2+(\beta_{00}^{yy} - \beta_{11}^{yy})(e^{\mu})-\beta_{10}^{yy}]\, M_y^{(N)} = 0$$

...(2.16b)

Equations (2.16a,b) are two homogeneous linear equations in $M_x^{(N)}$ and $M_y^{(N)}$ representing the condition of slope continuity.

For a non-trivial solution the determinant of the coefficients of equations (2.16a,b) must vanish. Hence we obtain the condition,

$$(\beta_{01}^{xx}\cdot(e^{\mu})^2 + (\beta_{00}^{xx}-\beta_{11}^{xx})\cdot(e^{\mu})-\beta_{10}^{xx})\cdot(\beta_{01}^{yy}\cdot(e^{\mu})^2+(\beta_{00}^{yy}-\beta_{11}^{yy})(e^{\mu})-\beta_{10}^{yy})$$

$$- (\beta_{01}^{xy}(e^{\mu})^2+(\beta_{00}^{xy}-\beta_{11}^{xy})(e^{\mu})-\beta_{10}^{xy})\cdot(\beta_{01}^{yx}(e^{\mu})^2+(\beta_{00}^{yx}-\beta_{11}^{yx})(e^{\mu})-\beta_{10}^{yx}) = 0$$

...(2.17a)

and

$$\frac{M_y^{(N)}}{M_x^{(N)}} = r(\mu) = -\frac{(\beta_{01}^{xx}(e^{\mu})^2+(\beta_{00}^{xx}-\beta_{11}^{xx})(e^{\mu})-\beta_{10}^{xx})}{(\beta_{01}^{xy}(e^{\mu})^2+(\beta_{00}^{xy}-\beta_{11}^{xy})(e^{\mu})-\beta_{10}^{xy})}$$

$$= -\frac{(\beta_{01}^{yx}(e^{\mu})^2+(\beta_{00}^{yx}-\beta_{11}^{yx})(e^{\mu})-\beta_{10}^{yx})}{(\beta_{01}^{yy}(e^{\mu})^2+(\beta_{00}^{yy}-\beta_{11}^{yy})(e^{\mu})-\beta_{10}^{yy})} \qquad \ldots(2.17b)$$

where, r is defined as the ratio of the out of phase moments at each support.

Equation (2.17a) is a fourth order polynomial in (e^{μ}) having real coefficients. The four roots of this equation e^{μ_i}, i=1,4 correspond to the four values of the propagation constant. Moment continuity has already been incorporated as discussed earlier. Also the constraint of zero displacement at the supports has been taken care of by using appropriate receptances (section 2.7). Since there exist four roots e^{μ_i}, i=1,4,for each μ_i, we obtain the eigen-vectors $M_{x,i}^{(N)}$ $M_{y,i}^{(N)}$ and an r_i such that

$$M_{y,i}^{(N)}/M_{x,i}^{(N)} = r_i = r(\mu_i),\ i = 1,4 \qquad \ldots(2.17c)$$

The moment components at the (N)'th support may be expressed in general as a linear combination of the eigen-vectors. Hence

$$M_x^{(N)} = M_{x,1}^{(N)} + M_{x,2}^{(N)} + M_{x,3}^{(N)} + M_{x,4}^{(N)} \qquad \ldots(2.18a)$$

$$M_y^{(N)} = M_{y,1}^{(N)} + M_{y,2}^{(N)} + M_{y,3}^{(N)} + M_{y,4}^{(N)}$$

$$= r_1 \cdot M_{x,1}^{(N)} + r_2 \cdot M_{x,2}^{(N)} + r_3 \cdot M_{x,3}^{(N)} + r_4 \cdot M_{x,4}^{(N)} \qquad \ldots(2.18b)$$

where, $M_{x,i}^{(N)}$, i=1,4 arefour unknown moments of the same phase at the Nth support.

Using equation (2.15a and b) we may relate the moments at the (N+1)th and (N)th support as,

$$\frac{M_{x,i}^{(N+1)}}{M_{x,i}^{(N)}} = \frac{M_{y,i}^{(N+1)}}{M_{y,i}^{(N)}} = e^{\mu_i}, \quad i = 1,4; \; N=0,\pm1,\pm2,\ldots$$

...(2.18d)

Therefore, in general at the (N+1)th support

$$M_x^{(N+1)} = M_{x,1}^{(N)}\cdot(e^{\mu_1}) + M_{x,2}^{(N)}\cdot(e^{\mu_2}) + M_{x,3}^{(N)}\cdot(e^{\mu_3}) + M_{x,4}^{(N)}(e^{\mu_4})$$

...(2.19a)

and

$$M_y^{(N+1)} = M_{y,1}^{(N)}(e^{\mu_1}) + M_{y,2}^{(N)}(e^{\mu_2}) + M_{y,3}^{(N)}(e^{\mu_3}) + M_{y,4}^{(N)}(e^{\mu_4})$$

$$= M_{x,1}^{(N)}\cdot r_1\cdot e^{\mu_1} + M_{x,2}^{(N)}\cdot r_2\cdot e^{\mu_2} + M_{x,3}^{(N)}\cdot r_3\cdot e^{\mu_3} + M_{x,4}^{(N)}\cdot r_3\cdot e^{\mu_4}$$

...(2.19b)

Thus we have satisfied the intermediate constraints by prescribing

(i) the propagation constants which relate the moments at different supports (equation (2.17a)),

(ii) the inter-relation between the out of phase moments at a support (equation (2.18c)).

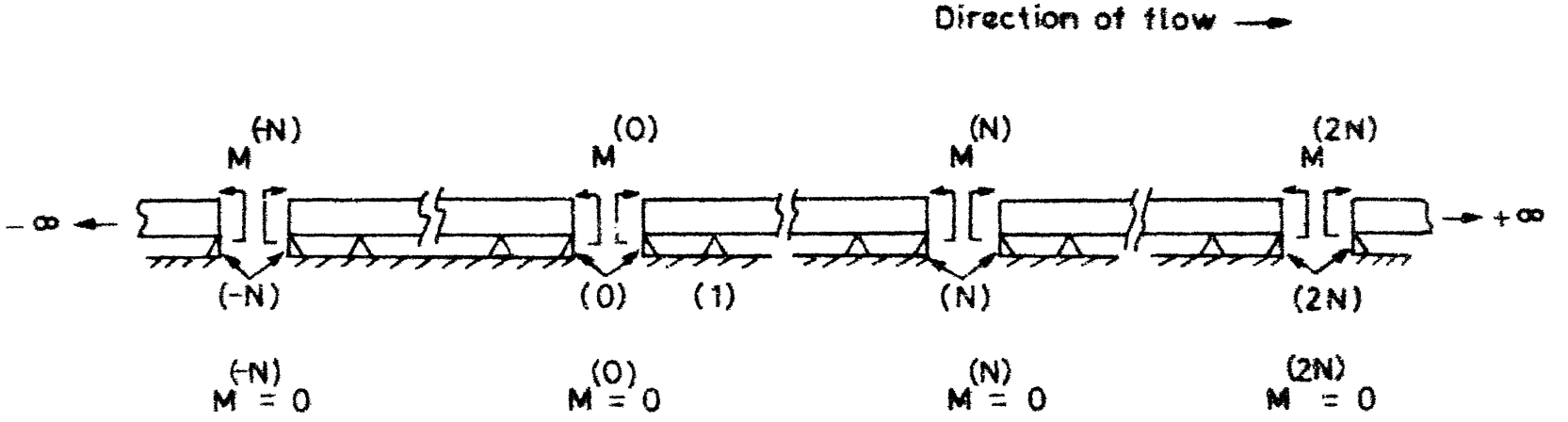

Fig. 2-3 An infinite pipe displayed as a periodic extension of a finite N-span pipe with zero end moments

For complete solution there remain only four unknowns i.e. $M^N_{x,1}$; $M^N_{x,2}$; $M^N_{x,3}$; $M^N_{x,4}$ yet to be determined. As shown in Fig. (2.3) if the infinite pipe under consideration were constrained to oscillate in such a fashion that the moments at the (0)th, ($\pm$N)th, ($\pm$2N)th.... supports were zero, the system would be equivalent to a periodic extension of a finite N-span pipe having zero end moments. Hence the method of propagation constants developed in this section may usefully be applied to obtain the bounding frequencies for a finite N-span pipe by imposing the condition of zero end moments.

2.5 Determination of Primary Instability Boundaries

In this section, we shall discuss the method of obtaining the principal primary instability boundaries of an N-span periodically supported pipe. In other words, we will seek those frequencies Ω_j, $j = 1,2,3\ldots$, (termed bounding frequencies) which will generate such propagation constants μ_i, $i = 1,4$ that cause the moments at the end supports to vanish.

Let $M^{(0)}$, $M^{(N)}$ denote the total moments at the extreme supports (see Fig. 2.3). Then using equations (2.18a, b,c) and (2.19a,b) we may write for $M^{(0)}$, $M^{(N)}$ as,

$$M^{(0)} = M_x^{(0)} \sin\left(\frac{\Omega t}{2}\right) + M_y^{(0)} \cos\left(\frac{\Omega t}{2}\right)$$

$$= (M_1 + M_2 + M_3 + M_4) \sin\left(\frac{\Omega t}{2}\right)$$

$$+ (M_1 \cdot r_1 + M_2 \cdot r_2 + M_3 \cdot r_3 + M_4 \cdot r_4) \cos\left(\frac{\Omega t}{2}\right) \qquad \ldots(2.20)$$

where for simplicity we denote

$$M_i = M_{x,i}^{(0)} .$$

At the Nth support

$$M_{x,i}^{(N)} = M_{x,i}^{(0)} \cdot (e^{\mu_i})^N = M_i \cdot (e^{\mu_i})^N \qquad \ldots(2.21a)$$

$$M_{y,i}^{(N)} = M_{y,i}^{(0)} \cdot (e^{\mu_i})^N = r_i \cdot M_i \cdot (e^{\mu_i})^N \; ; \; i=1,4 \; \ldots(2.21b)$$

Hence,

$$M^{(N)} = M_x^{(N)} \sin\left(\frac{\Omega t}{2}\right) + M_y^{(N)} \cos\left(\frac{\Omega t}{2}\right)$$

$$= [M_1 \cdot (e^{\mu_1})^N + M_2 \cdot (e^{\mu_2})^N + M_3 \cdot (e^{\mu_3})^N + M_4 \cdot (e^{\mu_4})^N] \sin\left(\frac{\Omega t}{2}\right)$$

$$+ [r_1 \cdot M_1 \cdot (e^{\mu_1})^N + r_2 \cdot M_2 \cdot (e^{\mu_2})^N + r_3 \cdot M_3 \cdot (e^{\mu_3})^N + r_4 \cdot M_4 \cdot (e^{\mu_4})^N] \cos\left(\frac{\Omega t}{2}\right)$$

...(2.22)

For zero end moments the coefficients of sine and cosine terms are separately equal to zero in equations (2.20) and (2.22). Therefore,

$$M_1 + M_2 + M_3 + M_4 = 0 \qquad \ldots(2.23a)$$

$$r_1 \cdot M_1 + r_2 \cdot M_2 + r_3 \cdot M_3 + r_4 \cdot M_4 = 0 \qquad \ldots(2.23b)$$

$$(e^{\mu_1})^N \cdot M_1 + (e^{\mu_2})^N \cdot M_2 + (e^{\mu_3})^N \cdot M_3 + (e^{\mu_4})^N \cdot M_4 = 0 \qquad \ldots(2.24a)$$

$$r_1 \cdot (e^{\mu_1})^N \cdot M_1 + r_2 \cdot (e^{\mu_2})^N \cdot M_2 + r_3 \cdot (e^{\mu_3})^N \cdot M_3 + r_4 \cdot (e^{\mu_4}) \cdot M_4 = 0 \qquad \ldots(2.24b)$$

For non-trivial solution, the determinant of the above system of equations must be equal to zero i.e.,

$$F(\Omega) = \begin{vmatrix} 1 & 1 & 1 & 1 \\ r_1 & r_2 & r_3 & r_4 \\ (e^{\mu_1})^N & (e^{\mu_2})^N & (e^{\mu_3})^N & (e^{\mu_4})^N \\ r_1 \cdot (e^{\mu_1})^N & r_2 \cdot (e^{\mu_2})^N & r_3 \cdot (e^{\mu_3})^N & r_4 \cdot (e^{\mu_4})^N \end{vmatrix} = 0 \quad \ldots(2.25)$$

The frequencies Ω_j, $j = 1, 2 \ldots$, where $F(\Omega) = 0$ correspond to the bounding frequencies of the instability zones.

The methodology used in the analysis may be summarized as follows. At the boundaries of the instability zones the system is governed by periodic solutions. For principal primary instability the solution is approximated as,

$$w(x,t) = X(x) \sin\left(\frac{\Omega t}{2}\right) + Y(x) \cos\left(\frac{\Omega t}{2}\right)$$

For such a form of the solution, we obtain receptances for a single span. Propagation constants are obtained by making use of the receptances and the constraints at the intermediate supports. By requiring the end moments to vanish we arrive at a constraint in terms of the propagation constants. Those frequencies at which this constraintis satisfied,correspond to the frequencies bounding the instability zones.

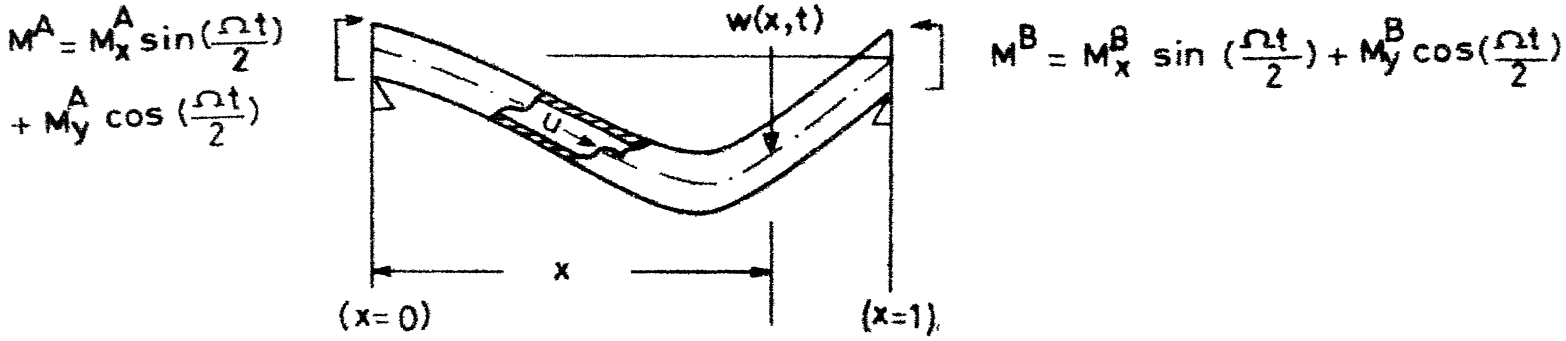

Fig. 2·4 Single span pipe conveying fluid used for receptance calculations

2.6 Determination of Receptances

In the previous analysis, sixteen different receptances are used to relate the slope and the internal moments at the supports. These receptances are obtained by solving for the response of a single span pipe subjected to four different combinations of harmonic end moments.

Consider a single span pipe as shown in Fig. (2.4) governed by the equations (2.08a and b). The displacement boundary conditions may be expressed as (see equation 2.08c),

$$X(0) = Y(0) = X(1) = Y(1) = 0 \quad \ldots(2.26)$$

Case I :

Let the system be acted upon by a unit sinusoidal moment at end A. Thus

$$M_A = 1 \cdot \sin\left(\frac{\Omega t}{2}\right)$$

$$M_B = 0$$

The dynamic response of the pipe, which is in linear proportion to the magnitude of the exciting moment, will be composed of an in phase and a quadrature component. The amplitude of the slope response at the two ends A and B, which is varying in phase with the sinusoidal moment at end A corresponds to the receptances β_{00}^{xx}, β_{10}^{xx}. Similarly the receptances β_{01}^{yx} and β_{10}^{yx}

are the quadrature components of the slope response at ends A and B respectively. Hence, one can write

$$\left(\frac{\partial w}{\partial x}\right)_A = \left(\frac{\partial X}{\partial x}\right)_A \sin\left(\frac{\Omega t}{2}\right) + \left(\frac{\partial Y}{\partial x}\right)_A \cos\left(\frac{\Omega t}{2}\right)$$

$$= \beta_{00}^{xx} \sin\left(\frac{\Omega t}{2}\right) + \beta_{00}^{yx} \cos\left(\frac{\Omega t}{2}\right)$$

and

$$\left(\frac{\partial w}{\partial x}\right)_B = \left(\frac{\partial X}{\partial x}\right)_B \sin\left(\frac{\Omega t}{2}\right) + \left(\frac{\partial Y}{\partial x}\right)_B \cos\left(\frac{\Omega t}{2}\right)$$

$$= \beta_{10}^{xx} \sin\left(\frac{\Omega t}{2}\right) + \beta_{10}^{yx} \cos\left(\frac{\Omega t}{2}\right)$$

The eight boundary conditions for this case are

$$X(0) = Y(0) = X(1) = Y(1) = 0 \qquad \ldots(2.26)$$

$$X''(0) = -M_x^A = -1 \qquad \ldots(2.27a)$$

$$Y''(0) = -M_y^A = 0 \qquad \ldots(2.27b)$$

$$X''(1) = -M_x^B = 0 \qquad \ldots(2.28a)$$

$$Y''(1) = -M_y^B = 0 \qquad \ldots(2.28b)$$

In the subsequent analysis we obtain a solution for this system of equations by the power series method.

Let,

$$X(x) = \sum_{m=0}^{K} g_m (1-x)^m \qquad \ldots(2.29a)$$

$$Y(x) = \sum_{m=0}^{K} h_m (1-x)^m \qquad \ldots(2.29b)$$

We substitute equations (2.29a and b) in (2.08a and b) and equate coefficients of like powers of (1-x) to zero. This translates the differential equations into the following recursive relations.

$$\frac{(m+4)!}{m!} g_{m+4} + \frac{(m+2)!}{m!} (a_2 - a_3) g_{m+2} - a_1 g_m - (m+1)(b_1 (m+1) - b_2) h_{m+1} = 0 \qquad \ldots(2.30a)$$

$$\frac{(m+4)!}{m!} h_{m+4} + \frac{(m+2)!}{m!} (a_2 + a_3) h_{m+2} - a_1 h_m - (m+1)(b_1 (m+1) + b_2) g_{m+1} = 0$$

$$m = 0,1,2\ldots., (K-4) \qquad \ldots(2.30b)$$

where, $a_1 = \frac{1}{4}\Omega^2$, $b_1 = \frac{\gamma}{2} u_o \Omega \delta$

$$a_2 = u_o^2 (1 + \frac{\delta^2}{2}), \quad b_2 = \gamma u_o \delta$$

and $a_3 = u_o^2 \delta$.

Substituting equations (2.29a and b) in equations (2.26, 2.27a and b, 2.28a and b) we may rewrite the boundary conditions as,

$$\sum_{m=0}^{K} g_m = \sum_{m=0}^{K} h_m = g_o = h_o = 0 \qquad \ldots(2.31)$$

$$\sum_{m=2}^{K} m(m-1)\, g_m = -M_x^A = -1 \qquad \ldots(2.32a)$$

$$\sum_{m=2}^{K} m(m-1)\, h_m = -M_x^A = 0 \qquad \ldots(2.32b)$$

$$2\, g_2 = -M_x^B = 0 \qquad \ldots(2.33a)$$

$$2\, h_2 = -M_y^B = 0 \qquad \ldots(2.33b)$$

The number of unknowns (g_o, g_1,...., g_K and h_o, h_1,....,h_K) totals to 2 (K+1). The set of two recursive relations (m = 0,1,2,..., (K-4)) generate 2 (K-3) equations and with 8 boundary conditions the total number of equations is 2 (K+1), and is equal to the number of unknowns.

Thus the problem has been reduced to finding a solution for the set of linear equations for which standard algorithms are available. Once the coefficients g_m, h_m; m=0,..,K have been computed we obtain the receptances from the following relations :

$$\beta_{00}^{xx} = \left(\frac{\partial X}{\partial x}\right)_{x=0} = \left[-\sum_{m=1}^{K} m\, g_m\, (1-x)^{m-1}\right]_{x=0} = -\sum_{m=1}^{K} m\, g_m \qquad \ldots(2.31a)$$

$$\beta_{00}^{yx} = \left(\frac{\partial Y}{\partial x}\right)_{x=0} = -\sum_{m=1}^{K} m\, h_m \qquad \ldots(2.31b)$$

$$\beta_{10}^{xx} = -\, g_1 \qquad \ldots(2.32a)$$

$$\beta_{10}^{yx} = -\, h_1 \qquad \ldots(2.32b)$$

Case II :

Let the end moments be

$$M_A = 1 \cdot \cos\left(\frac{\Omega t}{2}\right) \qquad \ldots(2.33a)$$

$$M_B = 0 \qquad \ldots(2.33b)$$

For such a case we obtain the following receptances

$$\beta_{00}^{xy} = X'(0) \qquad \ldots(2.34a)$$

$$\beta_{00}^{yy} = Y'(0) \qquad \ldots(2.34b)$$

$$\beta_{10}^{xy} = X'(1) \qquad \ldots(2.34c)$$

$$\beta_{10}^{yy} = Y'(1) \qquad \ldots(2.34d)$$

Case III and IV :

Following the method outlined for the earlier cases with $M^A = 0$ and $M^B = 1 \cdot \sin\left(\frac{\Omega t}{2}\right)$ we obtain β_{01}^{xx}, β_{01}^{yx}, β_{11}^{xx}, β_{11}^{yx} and with $M^A = 0$ and $M^B = 1 \cdot \cos\left(\frac{\Omega t}{2}\right)$ we obtain β_{01}^{xy}, β_{01}^{yy}, β_{11}^{xy}, β_{11}^{yy}.

It may be shown using reciprocity relations for dynamic receptances that,

$$\beta_{10}^{xx} = -\beta_{01}^{xx} \qquad \ldots(2.35a)$$

$$\beta_{00}^{yx} = \beta_{00}^{xy} \qquad \ldots(2.35b)$$

$$\beta_{10}^{yx} = -\beta_{01}^{xy} \qquad \ldots(2.35c)$$

$$\beta_{01}^{yx} = -\beta_{10}^{xy} \qquad \ldots(2.35d)$$

$$\beta_{11}^{yx} = \beta_{11}^{xy} \qquad \ldots(2.35e)$$

$$\beta_{10}^{yy} = -\beta_{01}^{yy} \qquad \ldots(2.35f)$$

2.7 Determination of Instability Bounds for the Uncoupled Case

It has been mentioned in section 2.3, that if the terms with the fluid mass ratio parameter, γ are neglected in equations (2.08a and b), the method for determining the

instability regions is considerably simplified. Such an approximation is valid when the fluid mass ratio, γ is much less with respect to the buckling ratio as defined below

$$\gamma \ll \phi < 1$$

where $\phi = \dfrac{(m_f \bar{U}_o^2)}{(\pi^2 EI/L^2)}$ and $\gamma = \left[\dfrac{m_f}{m_f + m_p}\right]^{1/2}$

In effect, by reducing $\gamma = 0$, we have neglected the terms arising due to

(i) coriolis acceleration and,

(ii) unsteady flow velocity with respect to the term in eqn.(2.03)($u^2 \dfrac{\partial^2 w}{\partial x^2}$) representing centrifugal effects.

It may be noted that the constraint on ϕ (the ratio between the equivalent axial load due to fluid flow with the first Euler buckling load) is less stringent. (All that is required is that $\phi < 1$).

Hence substituting $\gamma = 0$ in equations (2.08a and b) we obtain,

$$\frac{d^4X}{dx^4} + u_o^2 \left(1 - \delta + \frac{\delta^2}{2}\right) \frac{d^2X}{dx^2} - \frac{1}{4} \Omega^2 X = 0 \qquad \ldots(2.36a)$$

$$\frac{d^4Y}{dx^4} + u_o^2 \left(1 + \delta + \frac{\delta^2}{2}\right) \frac{d^2Y}{dx^2} - \frac{1}{4} \Omega^2 X = 0 \qquad \ldots(2.36b)$$

Equations (2.36a and b) are two uncoupled equations each representing simple transverse vibration of a beam with different axial loads. The frequency ($\frac{\Omega}{2}$) can be considered as the natural frequency of these beam columns. The calculations of receptances becomes easy since equations (2.36a and b) may be solved analytically. The cross receptances for this case will be zero and with reference to Fig. (2.4), the pipe slope at support B will be (see equations (2.11a and b)):

$$\theta_{Bx} = M_x^{(N)} \cdot \beta_{11}^{xx} + M_x^{(N-1)} \cdot \beta_{10}^{xx} \qquad \ldots(2.37a)$$

$$\theta_{By} = M_y^{(N)} \cdot \beta_{11}^{yy} + M_y^{(N-1)} \cdot \beta_{10}^{yy} \qquad \ldots(2.37b)$$

where, $\beta_{ij}^{xy} = \beta_{ij}^{yx} = 0 \qquad i = 0,1; \quad j = 0,1.$

By applying the condition for slope continuity in conjunction with equation (2.36a) we obtain a quadratic equation whose two roots e^{μ_1}, e^{μ_2} yield the propagation constants for X(x). In a similar manner equating $\theta_{By} = \theta_{Cy}$ we obtain another pair of propagation constants μ_3, μ_4 pertaining to Y(x) or the cosine component. For comparison with $\gamma \neq 0$ case it may be noted that in section 2.4 we had obtained a single fourth order polynomial in (e^{μ}) which yielded the four propagation constants. The fourth order polynomial of the propagation constants degenerates into two independent second order

polynomials in (e^{μ}) for the $\gamma = 0$ case. As in the case of a harmonic wave in an infinite periodic beam [9] in each set (μ_1, μ_2) and (μ_3, μ_4), the two propagation constants are of opposite sign. $(\mu_2 = -\mu_1$ and $\mu_4 = -\mu_3)$

To obtain the instability bounds for an N-span pipe we apply the zero end moments condition. Thus if $M^{(0)}_{y,1}$, $M^{(0)}_{y,2}$ $M^{(0)}_{x,1}$, $M^{(0)}_{x,2}$ are the unknown moments corresponding to μ_1, μ_2 respectively, at the (0)th support

$$M^{(0)} = M^{(0)}_x \sin\left(\frac{\Omega t}{2}\right) + M^{(0)}_y \cos\left(\frac{\Omega t}{2}\right)$$

$$= (M^{(0)}_{x,1} + M^{(0)}_{x,2}) \sin\left(\frac{\Omega t}{2}\right) + (M^{(0)}_{y,1} + M^{(0)}_{y,2}) \cos\left(\frac{\Omega t}{2}\right) \quad \ldots(2.38)$$

For $M^{(0)} = 0$ we obtain

$$M^{(0)}_{x,1} + M^{(0)}_{x,2} = 0 \quad \ldots(2.39)$$

$$M^{(0)}_{y,1} + M^{(0)}_{y,2} = 0 \quad \ldots(2.40)$$

At the Nth support in a like manner we obtain

$$M^{(N)}_{x,1} + M^{(N)}_{x,2} = 0 \quad \ldots(2.41a)$$

$$M^{(N)}_{y,1} + M^{(N)}_{y,2} = 0 \quad \ldots(2.41b)$$

Due to decoupling we may write the above equations as

$$M^{(0)}_{x,1} \cdot (e^{\mu_1})^N + M^{(0)}_{x,2} \cdot (e^{\mu_2})^N = 0 \qquad \ldots(2.42)$$

$$M^{(0)}_{y,1} \cdot (e^{\mu_3})^N + M^{(0)}_{y,2} \cdot (e^{\mu_4})^N = 0 \qquad \ldots(2.43)$$

Thus from equations (2.39) and (2.42) we obtain

$$\begin{bmatrix} 1 & 1 \\ (e^{\mu_1})^N & (e^{\mu_2})^N \end{bmatrix} \begin{Bmatrix} M^{(0)}_{x,1} \\ M^{(0)}_{x,2} \end{Bmatrix} = \{0\} \qquad \ldots(2.44)$$

For a non-trivial solution of equation (2.44)

$$((e^{\mu_1})^N - (e^{\mu_2})^N) = 0 \qquad \ldots(2.45)$$

Sengupta [10] has shown that for determination of natural frequencies only the propagating waves ($Re(\mu_1) = Re(\mu_2) = 0$) need to be considered. Equation (2.45) can be simplified to

$$Re(\mu_1) = 0 \qquad \ldots(2.46a)$$

$$Im(\mu_1) = \frac{m\pi}{N} \qquad m = 0,1,2,\ldots,N. \qquad \ldots(2.46b)$$

In a similar manner for the cosine component we obtain from equation (2.40 and 2.43)

$$\begin{bmatrix} 1 & 1 \\ (e^{\mu_3})^N & (e^{\mu_4})^N \end{bmatrix} \begin{Bmatrix} M_{y,1}^{(0)} \\ M_{y,2}^{(0)} \end{Bmatrix} = \{0\} \qquad \ldots(2.47)$$

which yields the condition.

$$\text{Re}\,(\mu_3) = 0 \qquad \ldots(2.48a)$$

$$\text{Im}\,(\mu_3) = \frac{m\pi}{N}\,, \quad m = 0,1,2,\ldots, N. \qquad \ldots(2.48b)$$

Frequencies within the propagation bands where conditions (2.46a,b and 2.48a,b) are fulfilled are the desired primary instability bounds. For each instability zone one bounding frequency is obtained from equation (2.46a and b) and the other from equation (2.48a and b). Equation (2.47b) (and also equation (2.48b)) can be solved by a simple graphical procedure presented in reference [10]. First a curve of $\text{Im}(\mu_1)$ versus Ω is drawn for the propagation band. Then by dividing the range of $\text{Im}(\mu_1)$ (0 to π) into N equal divisions, one obtains the natural frequencies in each band. As explained in references [9] and [10], the highest frequency in each band, as obtained by this method has to be discarded and thus one gets N natural frequencies from every propagation band. A similar procedure followed with the curve $\text{Im}(\mu_3)$ versus Ω yields the second set of N natural frequencies.

In the following analysis it is shown that for the case, $\gamma=0$ the method using the zero crossings of $F(\Omega)$ outlined in section 2.4 is equivalent to the graphical approach. For $\gamma = 0$, equations (2.08a and b) are uncoupled therefore

$$\beta^{xy}_{i,j} = \beta^{yx}_{i,j} = 0 \qquad i = 0,1 \ , \quad j = 0,1 \ .$$

Let e^{μ_1}, e^{μ_2} be one pair of conjugate roots, and e^{μ_3}, e^{μ_4} be the other pair. We redefine the ratio r_i such that the cross receptances appear in the numerator and the direct receptances in the denominator (for proper limiting).

Let

$$r'_i = \frac{M^{(N)}_{y,i}}{M^{(N)}_{x,i}} = -\frac{(\beta^{yx}_{01}\cdot(e^{\mu_i})^2 + (\beta^{yx}_{00} - \beta^{yx}_{11})\cdot(e^{\mu_i}) - \beta^{yx}_{10})}{(\beta^{yy}_{01}\cdot(e^{\mu_i})^2 + (\beta^{yy}_{00} - \beta^{yy}_{11})\cdot(e^{\mu_i}) - \beta^{yy}_{10})}$$

for $i = 1,2$. ...(2.49a)

and

$$r'_i = \frac{M^{(N)}_{x,i}}{M^{(N)}_{y,i}} = -\frac{(\beta^{xy}_{01}\cdot(e^{\mu_i})^2 + (\beta^{xy}_{00} - \beta^{xy}_{11})\cdot(e^{\mu_i}) - \beta^{xy}_{10})}{(\beta^{xx}_{01}\cdot(e^{\mu_i})^2 + (\beta^{xx}_{00} - \beta^{xx}_{11})\cdot(e^{\mu_i}) - \beta^{xx}_{10})}$$

for $i = 3,4$. ...(2.49b)

The condition of zero end moments equations (2.23a,b and 2.24a,b) in terms of r'_i, $i = 1,4$ becomes

$$M^{(0)}_{x,1} + M^{(0)}_{x,2} + r'_3 \cdot M^{(0)}_{y,3} + r'_4 \cdot M^{(0)}_{y,4} = 0 \qquad \ldots(2.50a)$$

$$(e^{N\mu_1}) \cdot M^{(0)}_{x,1} + (e^{N\mu_2}) \cdot M^{(0)}_{x,2} + r'_3 \cdot M^{(0)}_{y,3} \cdot e^{N\mu_3} + r'_4 \cdot M^{(0)}_{y,4} \cdot e^{N\mu_4} = 0 \qquad \ldots(2.50b)$$

$$r'_1 \cdot M^{(0)}_{x,1} + r'_2 \cdot M^{(0)}_{x,2} + M^{(0)}_{y,3} + M^{(0)}_{x,4} = 0 \qquad \ldots(2.51a)$$

$$r'_1 \cdot (e^{N\mu_1}) \cdot M^{(0)}_{x,1} + r'_2 \cdot (e^{N\mu_2}) \cdot M^{(0)}_{x,2} + (e^{N\mu_3}) \cdot M^{(0)}_{y,3} + (e^{N\mu_4}) \cdot M^{(0)}_{y,4} = 0 \qquad \ldots(2.51b)$$

which may be written in matrix form

$$\begin{bmatrix} 1 & 1 & r'_3 & r'_4 \\ e^{N\mu_1} & e^{N\mu_2} & r'_3 \cdot e^{N\mu_3} & r'_4 \cdot e^{N\mu_4} \\ r'_1 & r'_2 & 1 & 1 \\ r'_1 \cdot e^{N\mu_1} & r'_2 \cdot e^{N\mu_2} & e^{N\mu_3} & e^{N\mu_4} \end{bmatrix} \begin{Bmatrix} M^{(0)}_{x,1} \\ M^{(0)}_{x,2} \\ M^{(0)}_{y,3} \\ M^{(0)}_{y,4} \end{Bmatrix} = \{0\} \qquad \ldots(2.52)$$

In the limit of γ approaching zero, the cross receptances vanish i.e.,

$$\lim_{\gamma \to 0} r'_i = 0 \quad , \qquad i = 1,4 \qquad \ldots(2.53).$$

Hence

$$\begin{bmatrix} 1 & 1 & 0 & 0 \\ e^{N\mu_1} & e^{N\mu_2} & 0 & 0 \\ 0 & 0 & 1 & 1 \\ 0 & 0 & e^{N\mu_3} & e^{N\mu_4} \end{bmatrix} \begin{Bmatrix} M_{x,1}^{(0)} \\ M_{x,2}^{(0)} \\ M_{y,3}^{(0)} \\ M_{y,4}^{(0)} \end{Bmatrix} = \{0\} \quad \ldots(2.54)$$

where the system of equations has been decoupled into two sets of simultaneous equations which are identical to equations (2.44 and 2.47) obtained directly. As discussed in the following section, in the frequency regions where the coefficient matrix of equation (2.25) reduces to that of equation (2.54), one encounters computational problems.

2.8 Results and Discussions

2.8.1 Computations Performed

Using the analyses presented in the previous sections the following computations are performed:

(1) Curves for propagation constants versus frequency are obtained for $u_o = 0.6\pi$, $\delta = 0.3$, $\gamma = 0$ and $\gamma = 0.8$.

(2) The regions of principal primary instability are obtained with $u_o = 0.6\pi$ for the following values of the parameters in various cases.

Case (a): By direct method for one span pipe with $\gamma = 0.8$ and $\gamma = 0$ in the range of $\delta = 0.1$ to 0.5.

Case (b): By the propagation constants approach using $F(\Omega)$ for a one span pipe with the same values of the parameters as in (a).

Case (c): By the $F(\Omega)$ approach for a two span pipe with the same values of the parameters as in (a).

TABLE 2.1

Tabulation of convergence rate with truncation order K at different frequencies ($u_o = 0.6\pi$, $\gamma = 0.8$, $\delta = 0.3$).

Convergence Rate Parameter η^{*}; $\Delta K=4$

k	20	30	35	40	45	50
14	0.68	2.14	3.75	7.18	13.90	26.30
16	0.074	0.22	0.45	1.041	2.33	5.32
18	0.007	0.017	0.029	0.074	0.19	0.48

Convergence Rate Parameter η^{*}; $\Delta K=4$

K	50	70	90	100	110
20	0.04	0.5	9.0	8.36	-
24	0.00	0.006	0.117	0.12	2.14
28	0.00	0.00	0.00	0.001	0.04

$$\eta^{*} = 100 \left[\frac{\sum_{p,q,r,s} \left| \beta^{p,q}_{r,s}(K+\Delta K) - \beta^{p,q}_{r,s}(K) \right|}{\sum_{p,q,r,s} \left| \beta^{p,q}_{r,s}(K+\Delta K) \right|} \right]$$

where $\sum_{p,q,r,s}$ is summation over p=x,y; q=x,y; r=0,1; s=0,1;

and $\beta^{p,q}_{r,s}(K')$ is the receptance value evaluated with truncation order $K = K'$.

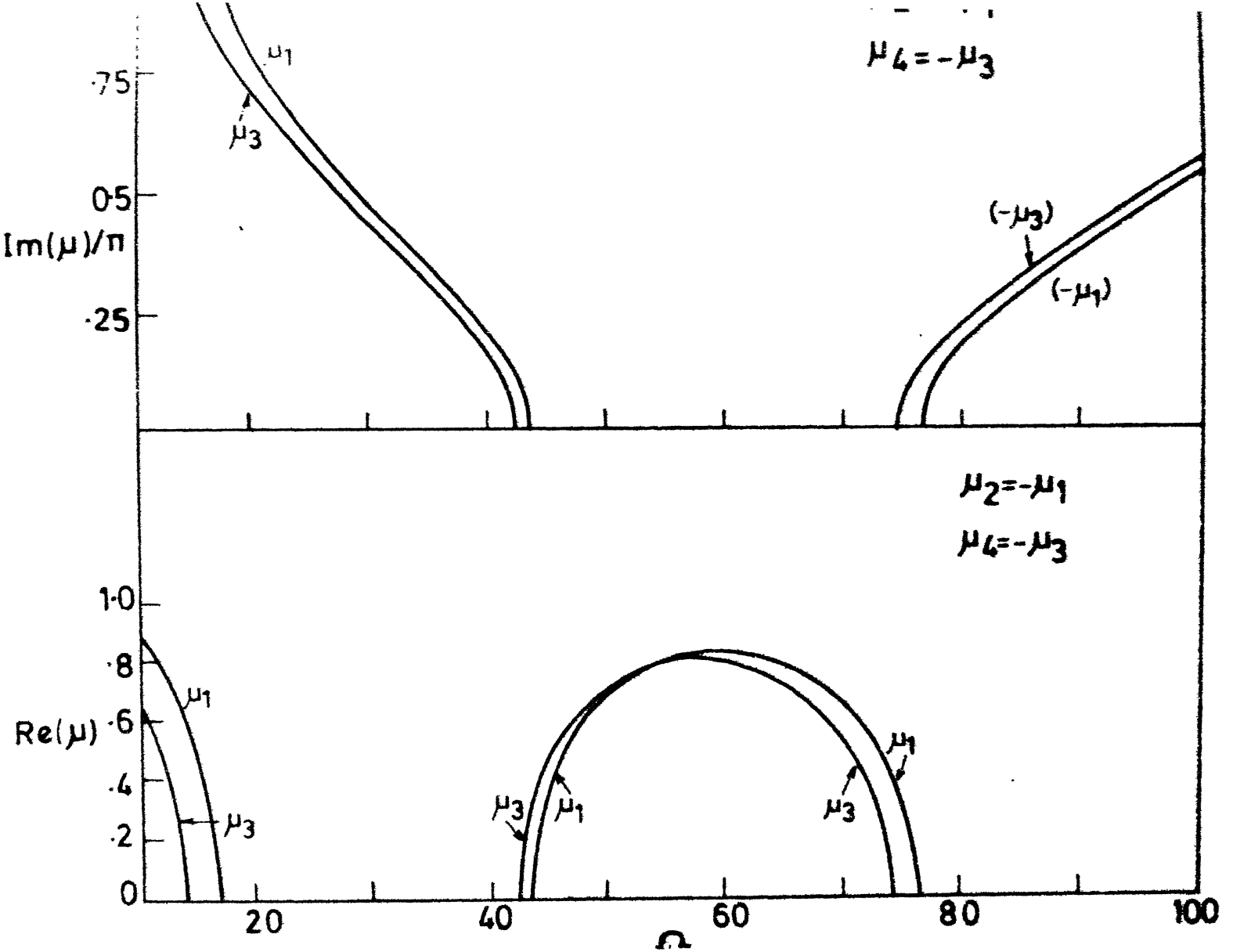

Fig 2·5 Propagation constants versus non dimensional frequency (uncoupled case) $\gamma=0$, $u_0=0{\cdot}6\,\pi$, $\delta=0{\cdot}3$

2.8.2 Discussions

The accuracy of the values for the receptances depends directly on the precision with which the truncated series solutions (equations (2.29a,b)) represent X(x) and Y(x). The rate of convergence in the receptance values with increasing number of terms in the power series solution is presented in Table (2.1). At higher frequencies we require larger number of terms. The convergence rate is relatively insensitive to other system parameters. Since most of the computation is involved in the frequency range of $\Omega = 0$ to $\Omega = 35$ for all calculations the series is truncated at K = 16. For computing the propagation constants in the range $\Omega = 10$ to $\Omega = 110$, K = 32 is used.

Figure (2.5) is a plot of the propagation constants μ_1 and μ_3 versus the non-dimensional frequency Ω for $u_o = 0.6\pi$, $\gamma = 0$, $\delta = 0.3$. For the uncoupled case ($\gamma = 0$), the propagation constants μ_i, i = 1,4 are observed to occur in pairs such that $\mu_1 = -\mu_2$, $\mu_2 = -\mu_3$ and $\mu_1 \neq \mu_3$. It is noted that μ_1, μ_3 is either purely real or purely imaginary as in the case of periodic beam [9]. Considering the curve for μ_1 (Fig.(2.5)) it is seen that in the range $\Omega = 0$ to $\Omega = 16.88$, μ_1 is purely real and this frequency interval is identified as the attenuation band [9]. At $\Omega = 16.88$ the real part goes to zero and over the interval $16.88 < \Omega < 43.3$, μ_1 is purely imaginary and varies from π to 0. This zone is termed as the propagation band since the waves associated with μ_1, μ_2 propagate without attenuation

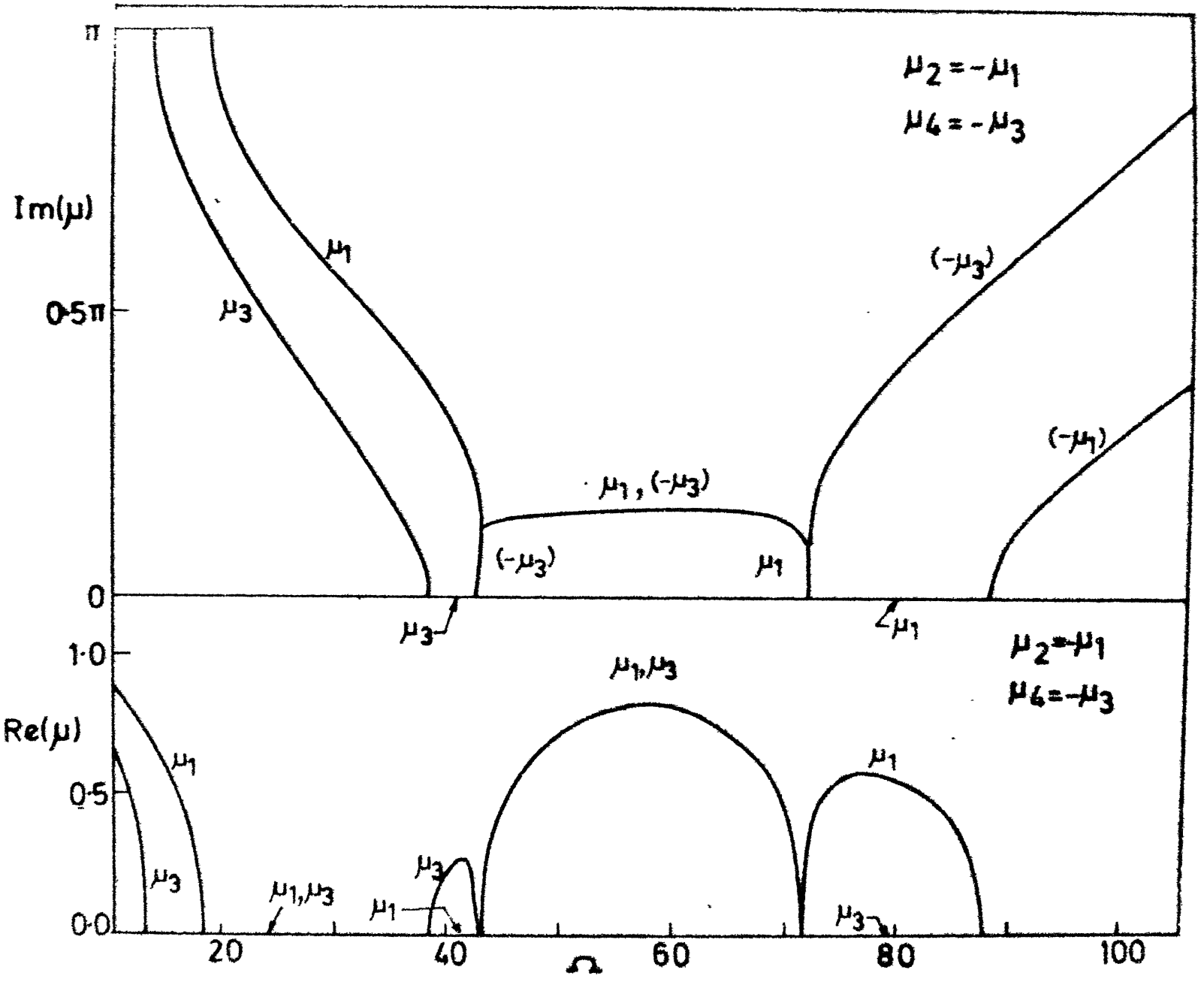

Fig. 2·6 Plot of propagation constants versus non dimensional frequency (coupled case) $\gamma = 0{\cdot}8$, $u_0 = 0{\cdot}6\pi$, $\delta = 0{\cdot}3$

The propagation band is followed by another attenuation band and so on, alternately, as Ω is increased. The propagation and attenuation bands for μ_3 follow the same pattern as μ_1. The plot for μ_3 is displaced on the frequency axis relative to that of μ_1, owing to the fact that the governing equations for X(x) and Y(x) even in the uncoupled case, are different (see equations (2.36 a,b)).

Based on the discussion in section 2.7 the instability bounding frequencies may be obtained directly from the plot of μ versus Ω. Thus for N = 2, one set of bounding frequencies are obtained at Re $(\mu_i) = 0$ and Im $(\mu_i) = \pi$, $i = 1$ and $i = 3$ i.e. the start of the respective propagation bands for μ_1 and μ_3. Similarly another set of frequencies for the second zone of instability are obtained with Re $(\mu_i) = 0$, Im $(\mu_i) = \frac{\pi}{2}$, $i = 1$ and $i = 3$. In general for an N span pipe there will be N principal primary zones of instability clustered together within each set of propagation bands. It will be seen later, that the first zone of instability always corresponds closely to the frequencies marking the start of the first propagation band of μ_1 and μ_3 for all values of γ and N.

When $\gamma \neq 0$ equations (2.08a,b) are coupled and the curves for propagation constants also change. Fig.(2.6) is a plot of μ_1 and μ_3 versus Ω for the case of high fluid mass ratio $\gamma = 0.8$ and $u_0 = 0.6\pi$, $\delta = 0.3$. We observe that between the first and second propagation bands, μ_1 and μ_3 are complex valued having both non-zero real and imaginary parts. Moreover,

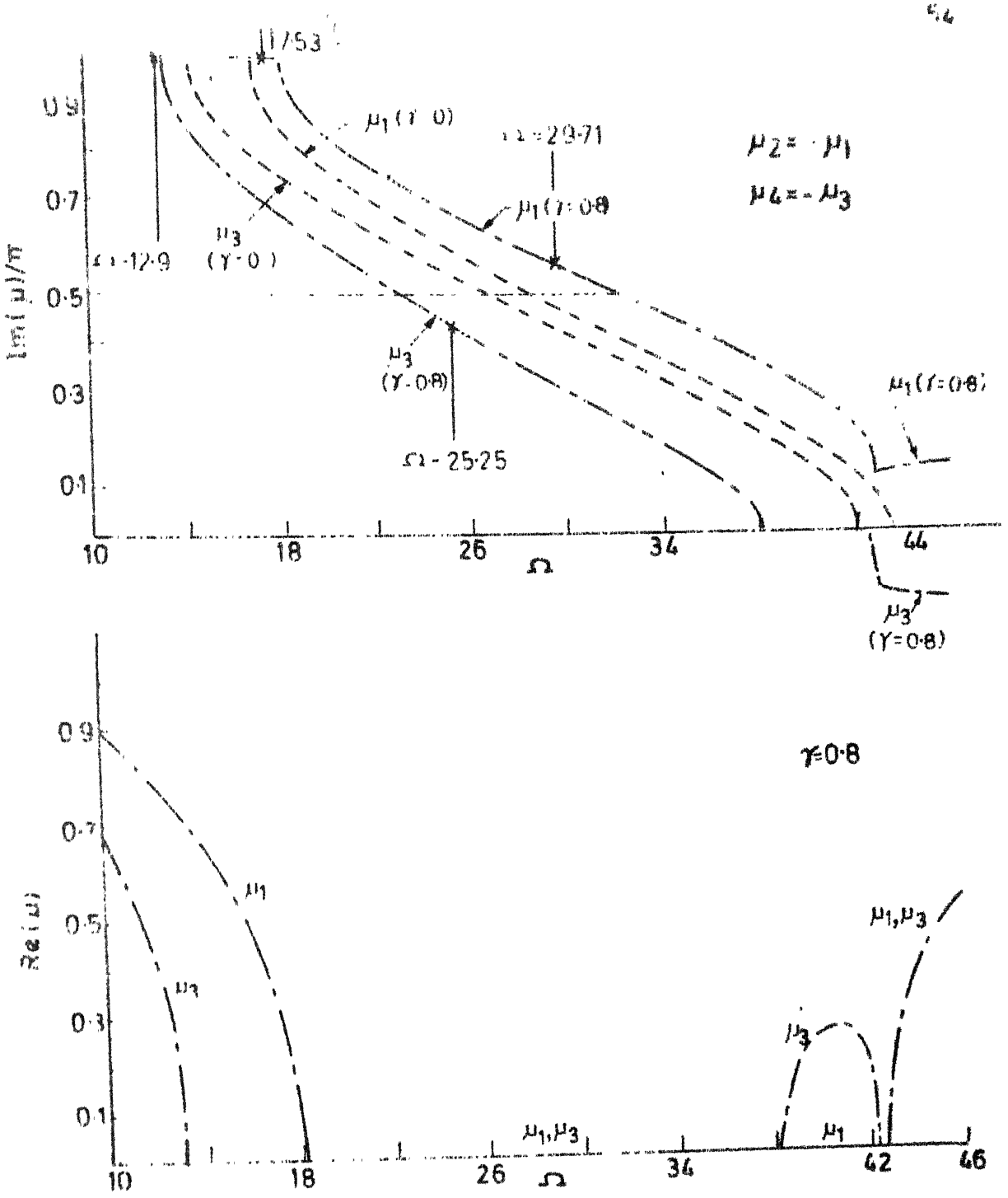

Fig 2·7 Curves showing μ versus frequency in the first propagation band $u_0 = 0.6\pi, \delta = 0.3$

TABLE 2.2

Values of Frequencies Bounding Principal Primary Instability Region for a Single Span Pipe, Obtained by Direct Evaluation of Frequency Determinant.

Trancation order : $K = 16$

Flow Velocity : $u_o = 0.6\pi$

Fluid Mass Ratio : $\gamma = 0$ (uncoupled case)

$\gamma = 0.8$ (coupled case)

FREQUENCIES

Excitation Parameter δ	$\gamma = 0$		$\gamma = 0.8$	
	Lower	Upper	Lower	Upper
0.01	15.747	15.836	15.347	15.506
0.10	15.318	16.208	14.614	16.203
0.20	14.782	16.572	13.766	16.945
0.30	14.177	16.887	12.881	17.650
0.40	13.492	17.155	11.955	18.319
0.50	12.716	17.378	10.982	18.950

in this frequency range $\mu_1 = \mu_3^*$ (i.e. μ_1 and μ_3 occur as conjugate pairs). As in the earlier case the set of μ_i, $i = 1,4$ remains closed under the unary operation (i.e. $\mu_1 = -\mu_2$ and $\mu_3 = -\mu_4$) at all frequencies.

Figure (2.7) is a plot of μ_1, μ_3 over the first propagation band for $\gamma = 0.8$ and $\gamma = 0$ with $u_o = 0.6\pi$, $\delta = 0.3$. On comparing curves of μ_1 and μ_3 for $\gamma = 0$ and $\gamma = 0.8$ we observe that the effect of increased coupling is to magnify the relative shift between the curves of μ_1 and μ_3. Increased separation between μ_1 and μ_3 plots indicates broadening of the instability zones as will be evident shortly.

The validity of the graphical approach in determining the instability bounds is restricted only to the uncoupled case (i.e. $\gamma = 0$). To obtain the instability bounds for the coupled case ($\gamma \neq 0$) we take resort to equation (2.25).

The frequency bounds for a single span pipe are first obtained for both the coupled and uncoupled case by the direct method mentioned in section 2.3. Table (2.2) is a list of these results for $u_o = 0.6\pi$, $\gamma = 0.8$ and $\gamma = 0$, $N = 1$. These frequencies closely correspond to the start of the propagation band of μ_1 and μ_3. For the particular case of $\delta = 0.3$ this may be compared by tallying the pair of frequencies in Table (2.2) with Fig. (2.7). The results obtained by this method are in excellent agreement with those obtained in reference [7] where the Ritz-Galerkin approach was used.

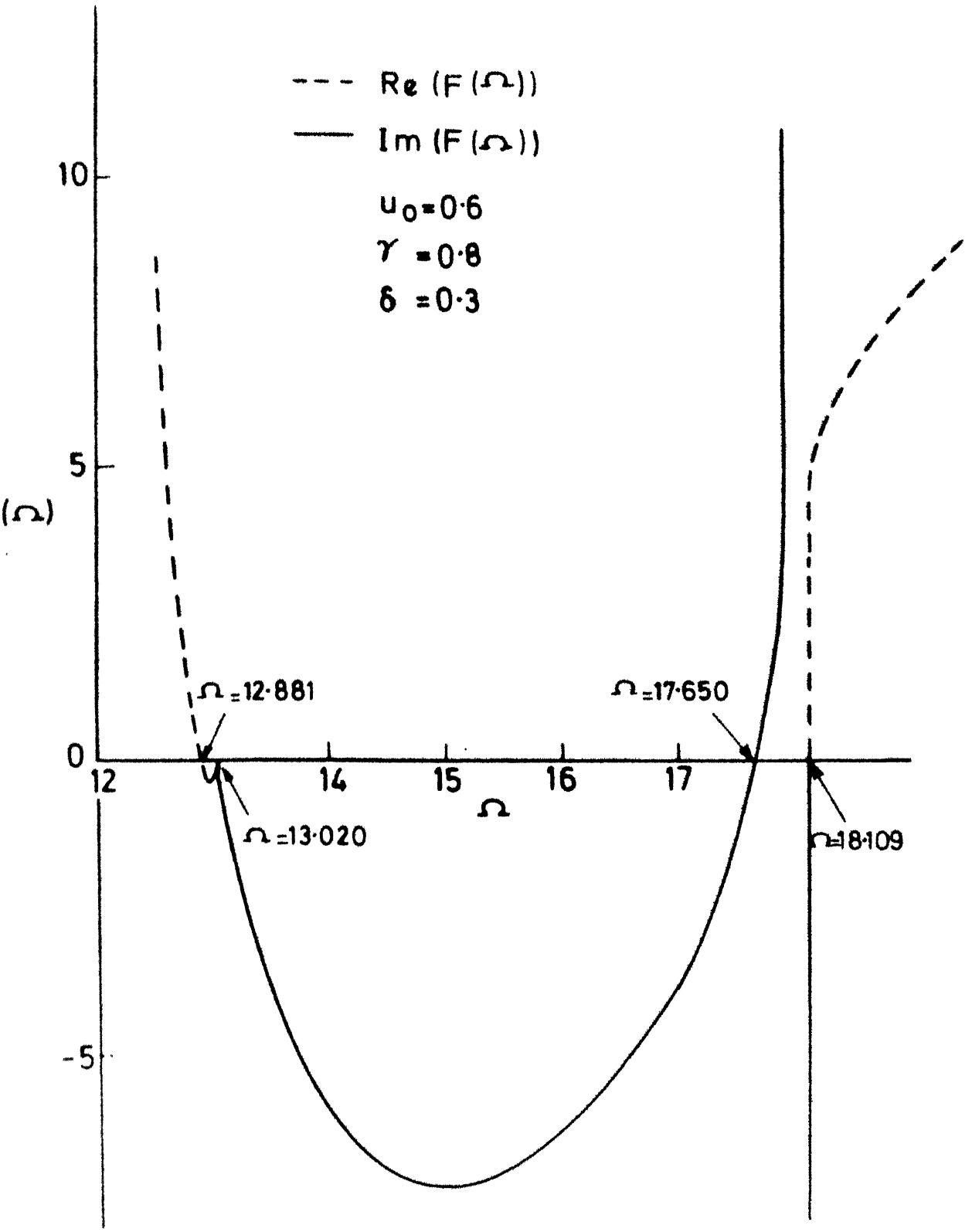

Fig.2·8 Plot of the determinant F(Ω) versus Ω for u_0 0·6 π, γ=0·8, δ - 0·3, N 1

TABLE 2.3

Values of Frequencies Bounding Principal Primary Instability Region for a Single Span Pipe, Obtained by Using Propagation Constants and the Determinant $F(\Omega)$.

Trancation order : $K = 16$

Flow Velocity : $u_o = 0.6\pi$

Fluid Mass Ratio : $\gamma = 0$ (uncoupled case)

$\gamma = 0.8$ (coupled case)

FREQUENCIES

Excitation Parameter δ	$\gamma = 0$		$\gamma = 0.8$	
	Lower	Upper	Lower	Upper
0.01	15.75	18.84	15.35	15.51
0.10	15.32	16.21	14.61	16.20
0.20	14.78	15.57	13.77	16.95
0.30	14.177	16.887	12.881	17.650
0.40	13.49	17.16	12.00	18.32
0.50	12.72	17.38	10.98	18.95

In the frequency determinant approach, the bounding frequencies are obtained by searching for the zero crossings of $F(\Omega)$ (equation (2.25)). To this end $F(\Omega)$ is plotted against Ω and a sample plot is shown in Fig. (2.8) for $u_o = 0.6\pi$, $\delta = 0.3$, $N = 1$, $\gamma = 0.8$. It is observed that at any frequency, Ω the function $F(\Omega)$ is either purely real or purely imaginary. The function exhibits zero crossings of the following types:

(1) $F(\Omega)$ remains purely real or purely imaginary in the vicinity of Ω_j where

$$F(\Omega_j) = 0.$$

(2) $F(\Omega)$ changes phase from real to imaginary or vice-versa as it changes sign across the point $\Omega = \Omega_j$ where

$$F(\Omega_j) = 0.$$

At the frequencies, $\Omega = 12.881$ and 17.650 the function exhibits zero crossings of the first kind and at $\Omega = 13.02$ and 18.109 zero crossings are of the second kind.

On comparing these frequencies with those obtained by the direct method for the same set of parameters (Table (2.2)), we infer that only the zero crossings of the first kind correspond to the bounding frequencies. The zeroes of the second kind exist due to some numerical problem discussed later in this section. Table (2.3) lists the results obtained by this method for $N=1$, $u_o = 0.6\pi$, $\gamma=0$, 0.8. These results tally exactly with the values in Table (2.2).

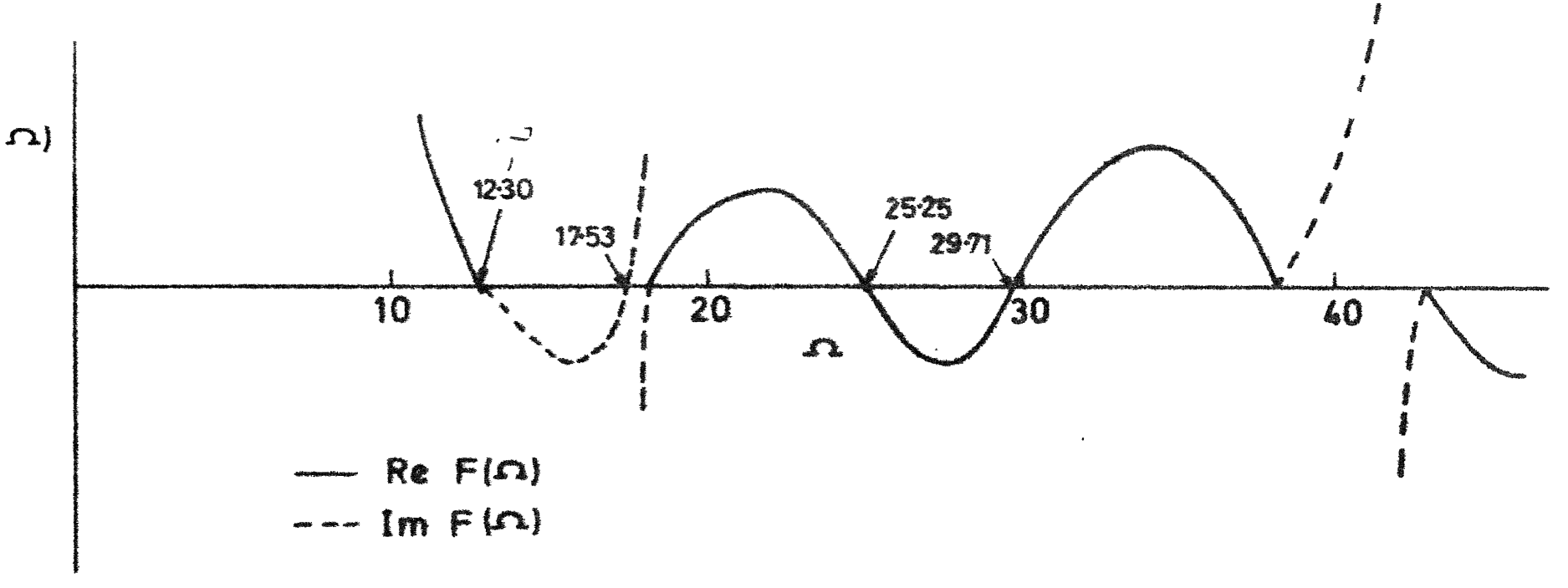

Fig 2·9 SKetch of $F(\Omega)$ versus Ω for $N=2$, $u_0=0{\cdot}6\ \pi$, $\gamma=0{\cdot}8$, $\delta=0{\cdot}3$

Figure (2.9) is a representative sketch of $F(\Omega)$ versus Ω for $N = 2$ with $u_o = 0.6\pi$, $\gamma = 0.8$, $\delta = 0.3$. The first pair of zero crossings (first kind) in this figure at $\Omega = 12.90$, and $\Omega = 17.53$ yield the bounding frequencies for the first zone of instability. With reference to Fig. (2.7), these frequencies closely correspond to the start of the propagation bands for μ_1 and μ_3 ($\gamma = 0.8$). Thus for the first zone even for $\gamma = 0.8$, the results are close to those obtained by the graphical approach

The second set of zero crossings in Fig. (2.9) at $\Omega = 25.25$ and $\Omega = 29.71$ correspond to the second zone of instability. At these frequencies,

$$\text{Re}\ (\mu_1) = \text{Re}\ (\mu_3) = 0$$

but

$$\text{Im}\ (\mu_1) \neq \pi/2 \neq \text{Im}\ (\mu_3)$$

which indicates that the graphical approach cannot be used to evaluate the second (or higher) zone of instability for $\gamma \neq 0$.

From this discussion we may conclude that the first zone of instability bounds always occur close to the start of the respective propagation bands for μ_1 and μ_3. This is regardless of the number of spans in the structure or the degree of coupling between $X(x)$ and $Y(x)$, as concluded in reference [12] For $\gamma \neq 0$ case, the higher zones however cannot be obtained by the graphical approach as concluded in reference [12]. These zones may be evaluated accurately only by using equation (2.25).

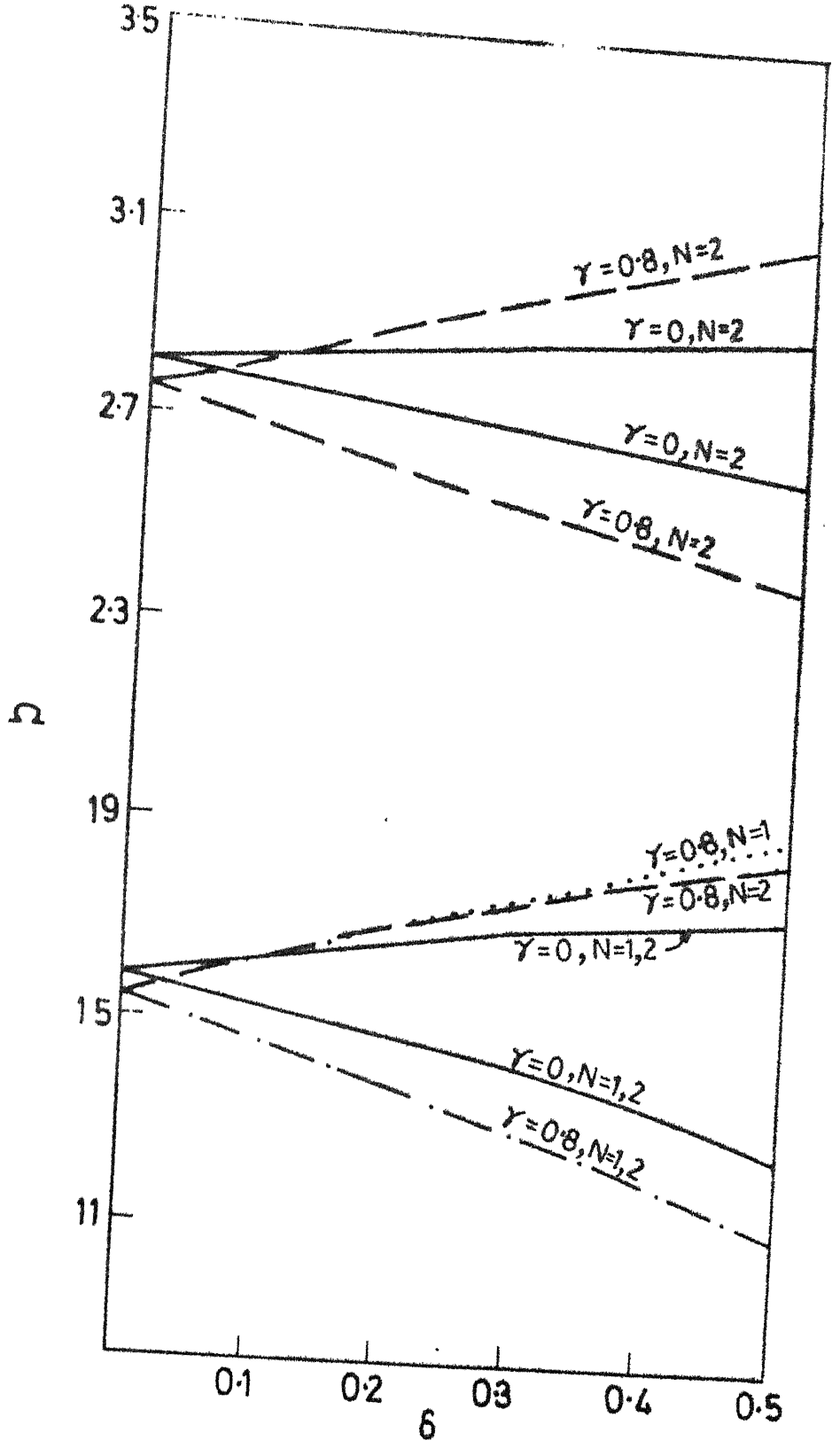

Fig. 2·10 Regions of principal primary instability for $u_0 = 0{\cdot}6\pi, \gamma = 0, 0{\cdot}8, N = 1, 2$

It is shown in section 2.7 that the graphical approach applies when the matrix in equation (2.52) becomes decoupled. The fact that at the bounds of the first instability zone, the graphical approach and the frequency determinant approach, give identical results suggests, that at these frequencies equation (2.52) is effectively decoupled. This implies that even for $\gamma = 0.8$, $r_i' = 0, (i = 1,4)$ near the start of the propagation bands of μ_1 and μ_3. In other words cross receptances are very small in comparison to the direct receptances at these two frequencies. However the importance of the cross receptances while calculating the propagation constants is easily seen from the considerable change in the pair of curves (μ_1, μ_3) for the two cases $\gamma = 0.8$ and $\gamma = 0$ as shown in Fig. (2.7).

In the vicinity of the boundaries of the first zone, since r_i' 's approach zero, irrespective of the value of γ, the determinant $F(\Omega)$ becomes ill conditioned with one or more rows having very small numbers in comparison to the other rows. This results in the spurious zeroes (zero crossings of the second kind) mentioned earlier. No spurious zeroes were encountered near the bounds for the higher instability zones. Also these results are significantly different from those obtained by graphical approach, indicating the increased importance of the cross receptance for these zones.

Figure (2.10) is a plot of the instability zones in the $\Omega - \delta$, plane for $N = 1,2$, $\gamma = 0$, 0.8 and $u_o = 0.6\pi$.

TABLE 2.4

Values of frequencies bounding the principal primary instability regions associated with the first two modes of a two span pipe (using propagation constants and determinant $F(\Omega)$). $K = 16$, $u_o = 0.6\pi$

Frequencies Ω (Uncoupled case $\gamma = 0$)

Excitation Parameter δ	I mode		II mode	
	Lower	Upper	Lower	Upper
0.01	15.747	15.836	28.023	28.082
0.10	15.318	16.208	27.743	28.330
0.20	14.782	16.572	27.399	28.576
0.30	14.177	16.887	27.020	28.791
0.40	13.493	17.455	26.604	28.976
0.50	12.716	17.378	25.149	29.132

Frequencies Ω (coupled case $\gamma = 0.8$)

Excitation Parameter δ	I mode		II mode	
	Lower	Upper	Lower	Upper
0.01	15.348	15.598	27.463	27.612
0.10	14.625	16.183	26.773	28.289
0.20	13.781	16.887	26.006	29.017
0.30	12.897	17.528	25.254	29.714
0.40	11.969	18.083	24.540	30.374
0.50	10.994	18.516	23.905	30.993

In the range of frequencies considered we observe one and two instability zones for N = 1 and 2 respectively. From these curves we conclude that the width of the instability zones for both $\gamma = 0.8$, $\gamma = 0$ increases with δ. On increasing γ, from 0 to 0.8 the instability zones become broader and this difference is seen to be greater for higher δ's. In the low δ region (0 - 0.1) it is observed that increasing γ shifts the zone to lower frequencies. These conclusions are at a variance from those obtained in [5]and[12] where it was observed that the effect of increasing γ is to depress the instability zones uniformly to lower frequencies and that this change is less for higher values of δ. The errors in reference [12] arise due to

i) Improper analysis at the stage of obtaining the propagation constants.

ii) Improper equations in deriving the end moment conditions.

iii) Use of a different governing equation based on reference [6] which itself is erroneous as shown in reference [7].

Numerical values for the two span pipe for $u_o = 0.6\pi$, $\gamma = 0, 0.8$ are presented in Table (2.4).

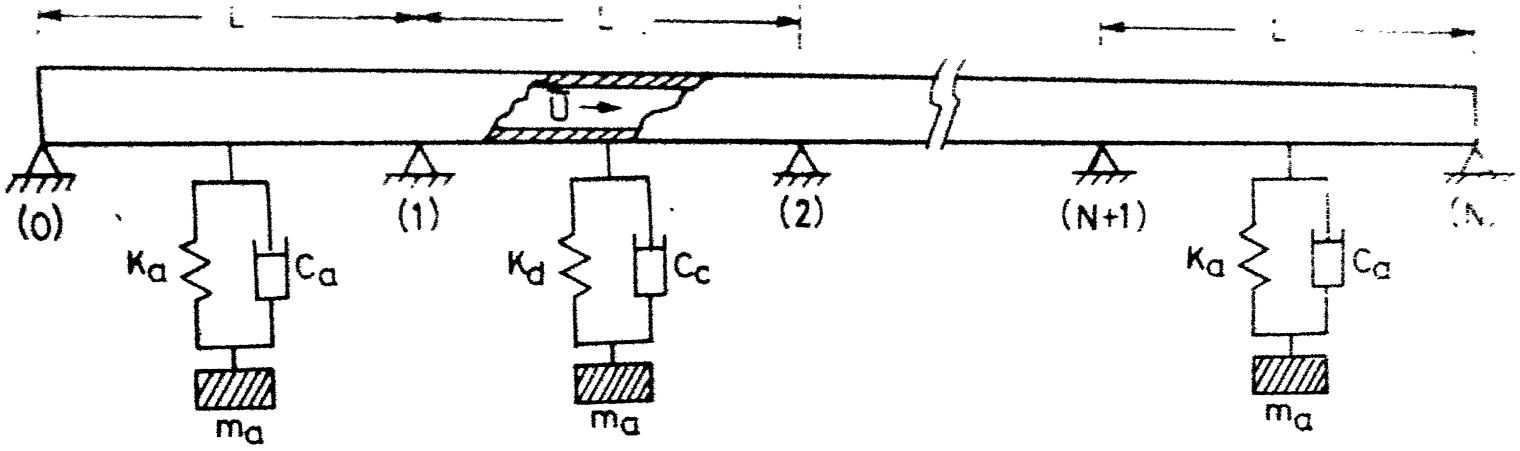

Fig. 3-1a Periodically supported N-span pipe with absorbers

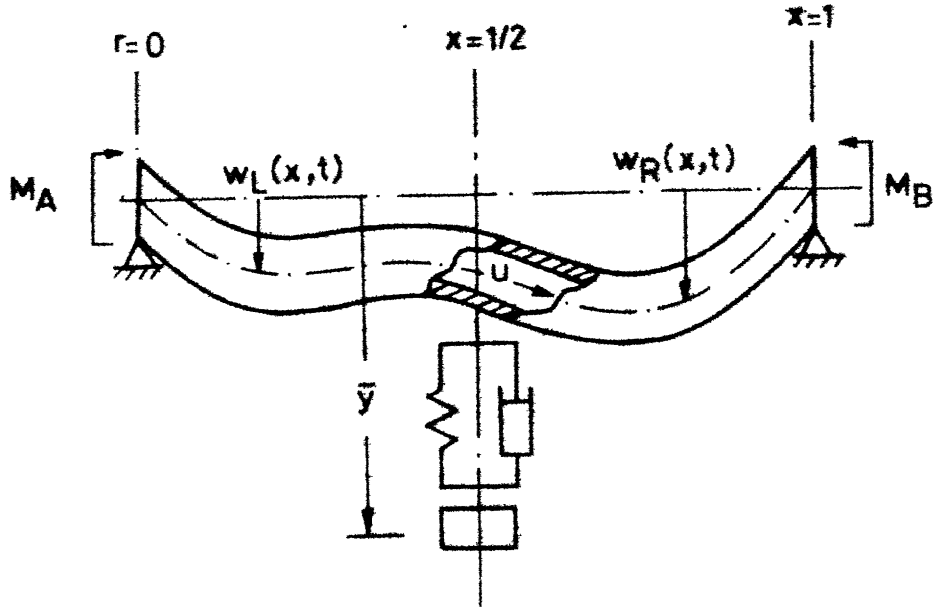

Fig. 3-1b Periodic pipe element used for receptance calculations

CHAPTER - III

CONTROL OF PARAMETRIC INSTABILITIES BY DYNAMIC ABSORBERS

3.1 Introduction

Dynamic absorbers are used to control the excessive vibrations in mechanical systems. By suitably varying the absorber parameters, the system impedance can be changed accordingly. Unlike dampers which reduce the system response by dissipating energy, an undamped absorber diminishes the response by force cancellation. A dynamic absorber normally consists of a lumped mass that is attached to the main (or primary) system by a damped resilient element.

In the present chapter, a viscously damped dynamic absorber has been tried for a different use from its conventionalrole of reducing the resonant motion. The aim of the present study is to determine whether the dynamic absorber can effectively control the regions of parametric instabilities of a pipe.

As stated in Chapter - II in most of the cases, the principal region of instability is of primary importance. The fluid mass ratio parameter, γ has been retained since it has been found to influence the primary zones significantly (Section 2.8). To maintain the periodicity in the overall structure, the absorber need be attached at identical location in each span. In the present work, the point of attachment of

the absorber is taken as the mid-point of each bay. Computations have been performed for N = 2 only, though the method used is equally valid for any number of spans. The elegance of the method lies in the fact that only the matrix used in Chapter-II for receptance calculation need be changed. The rest of the computation is on identical lines with the case without the absorber.

3.2 Equations of Motion and Receptances

Consider a pipe of N-spans, each having a length L resting on line supports (as discussed in chapter-II). A viscously damped absorber of mass m_a, spring constant k_a and viscous damping coefficient C_a is attached to the mid-point of each span (Fig.(3.1a)). The periodic element for this structure is shown in Fig. (3.1b). Let $\bar{w}_L(x,t)$ and $\bar{w}_R(x,t)$ refer to the transverse displacement of the left (x = 0 to 1/2) half and the right half (x = 1/2 to 1) respectively, of the pipe element.

We shall proceed first to derive the boundary conditions at $\bar{x} = 1/2$ imposed by the addition of the absorber. The displacement, slope and moment continuity relations across the absorber are,

$$\bar{w}_L\left(\frac{L}{2}, \tau\right) = \bar{w}_R\left(\frac{L}{2}, \tau\right) \qquad \ldots(2.55a)$$

$$\frac{\partial \bar{w}_L}{\partial \bar{x}} \left(\frac{L}{2}, \tau \right) = \frac{\partial \bar{w}_R}{\partial \bar{x}} \left(\frac{L}{2}, \tau \right) \qquad \ldots(2.55b)$$

$$\frac{\partial^2 \bar{w}_L}{\partial \bar{x}^2} \left(\frac{L}{2}, \tau \right) = \frac{\partial^2 \bar{w}_R}{\partial \bar{x}^2} \left(\frac{L}{2}, \tau \right) \qquad \ldots(2.55c)$$

Following a non-dimensionalising scheme as in section 2.2 we may rewrite equations (2.55a,b and c) as

$$w_L \left(\tfrac{1}{2}, t \right) = w_R \left(\tfrac{1}{2}, t \right) \qquad \ldots(2.56a)$$

$$w_L' \left(\tfrac{1}{2}, t \right) = w_R' \left(\tfrac{1}{2}, t \right) \qquad \ldots(2.56b)$$

$$w_L'' \left(\tfrac{1}{2}, t \right) = w_R'' \left(\tfrac{1}{2}, t \right) \qquad \ldots(2.56c)$$

where w_L and w_R are the non-dimensional equivalents of $\bar{w}_L$ and $\bar{w}_R$, respectively.

For the K = 1 approximation (section 2.3) we may write

$$w_L = X_L \sin \left(\tfrac{1}{2} \Omega t \right) + Y_L \cos \left(\tfrac{1}{2} \Omega t \right) \qquad \ldots(2.57a)$$

$$w_R = X_R \sin \left(\tfrac{1}{2} \Omega t \right) + Y_R \cos \left(\tfrac{1}{2} \Omega t \right) \qquad \ldots(2.57b)$$

Using equations (2.56a,b,c) and (2.57a,b) we obtain

$$X_L \left(\tfrac{1}{2} \right) = X_R \left(\tfrac{1}{2} \right) \qquad \ldots(2.58a)$$

$$X_L' \left(\tfrac{1}{2} \right) = X_R' \left(\tfrac{1}{2} \right) \qquad \ldots(2.58b)$$

$$X_L''\left(\frac{l}{2}\right) = X_R''\left(\frac{l}{2}\right) \qquad \ldots(2.58c)$$

$$Y_L\left(\frac{l}{2}\right) = Y_R\left(\frac{l}{2}\right) \qquad \ldots(2.58d)$$

$$Y_L'\left(\frac{l}{2}\right) = Y_R'\left(\frac{l}{2}\right) \qquad \ldots(2.58e)$$

$$Y_L''\left(\frac{l}{2}\right) = Y_R''\left(\frac{l}{2}\right) \qquad \ldots(2.58f)$$

The shear force balance at $x = \frac{l}{2}$ yields the fourth coupling relation between w_L and w_R. Let $\bar{V}_R$ and $\bar{V}_L$ be the shear forces in the pipe at the right and left of the absorber location (at $\bar{x} = 1/2$). Then

$$\bar{V}_L = EI \frac{\partial^3 \bar{w}_L}{\partial \bar{x}^3}\left(\frac{L}{2}, \tau\right) \qquad \ldots(2.59a)$$

$$\bar{V}_R = EI \frac{\partial^3 \bar{w}_R}{\partial \bar{x}^3}\left(\frac{L}{2}, \tau\right) \qquad \ldots(2.59b)$$

Let $\bar{y}$ be the independent coordinate describing the transverse displacement of the absorber mass (Fig. (3.1b)).

Balancing the shear forces at $\bar{x} = \frac{L}{2}$, together with the equation of motion for m_a, we obtain

$$\bar{V}_R - \bar{V}_L = \left[K_a (\bar{y} - \bar{w}_L) + C_a \left(\frac{d\bar{y}}{d\tau} - \frac{\partial}{\partial \tau} \bar{w}_L\right)\right]_{\bar{x} = L/2} \qquad \ldots(2.60a)$$

and $$\bar{V}_R - \bar{V}_L = - m_a \frac{d^2 y}{\quad 2} \qquad \ldots(2.60b)$$

Eliminating V_R, V_L and $\bar{y}$ from equations (2.59a,b) and (2.60a,b) we obtain

$$EI \frac{\partial^3}{\partial \bar{x}^3} \left[m_a \ddot{\bar{w}}_R + C_a \dot{\bar{w}}_R + K_a \bar{w}_R \right] = EI \frac{\partial^3}{\partial \bar{x}^3} \left[m_a \ddot{\bar{w}}_L + C_a \dot{\bar{w}}_L + K_a \bar{w}_L \right] - m_a \left[K_a \ddot{\bar{w}}_L + C_a \dddot{\bar{w}}_L \right], \text{ at } \bar{x} = L/2 \quad \ldots(2.61)$$

where $(\dot{})$ denotes derivative with respect to time, τ.

Expressing above equation in a non-dimensional form, we obtain

$$\frac{\partial^3}{\partial x^3} \left[\ddot{w}_R + \zeta_a \sigma_a^2 \pi^4 \dot{w}_R + \sigma_a^2 \pi^4 w_R \right] = \frac{\partial^3}{\partial x^3} \left[\ddot{w}_L + \zeta_a \sigma_a^2 \pi^4 \dot{w}_L + \sigma_a^2 \pi^4 w_L \right] - \sigma_a^2 \pi^4 r_a \left[\zeta_a \dddot{w}_L + \ddot{w}_L \right], \text{ at } x = 1/2 \quad \ldots(2.62)$$

where $(\,) = \frac{\partial}{\partial t}$, non-dimensional time derivative,

$$\zeta_a = \frac{C_a}{\sigma_a \pi^2 \sqrt{K_a m_a}}, \text{ the damping factor.}$$

$$\sigma_a = \frac{\omega_a^2}{\pi^2} \left[\frac{K_a (m_f + m_p)}{m_a EI} \right]^{1/2}, \text{ the tuning ratio,}$$

$$r_a = \frac{m_a}{(m_f + m_p) L}, \text{ the absorber mass ratio.}$$

Substituting the expressions for w_R and w_L from equations (2.57a, b) in above equation we get,

$$\begin{bmatrix} C_1 & -C_1 \\ C_2 & -C_2 \end{bmatrix} \begin{Bmatrix} X_L''' \\ X_R''' \end{Bmatrix} + \begin{bmatrix} -C_2 & +C_2 \\ C_1 & -C_1 \end{bmatrix} \begin{Bmatrix} Y_L''' \\ Y_R''' \end{Bmatrix}$$

$$+ \begin{bmatrix} D_1 & -D_2 \\ -D_2 & D_1 \end{bmatrix} \begin{Bmatrix} X_L \\ Y_L \end{Bmatrix} = \begin{matrix} 0 \\ 0 \end{matrix}$$

$$x = 1/2, \qquad \ldots(2.63)$$

where

$$C_1 = \left[1 - \frac{\Omega^2}{4\sigma^2 \pi^4} \right], \quad D_1 = r_a \frac{\Omega^2}{4}$$

$$C_2 = \frac{\Omega \zeta_a}{2}, \quad D_2 = \zeta_a \, r_a \frac{\Omega^3}{8}$$

Equations (2.58a, b, c, d, e, f) and (2.63) are the eight equations which couple the solutions in the right and left half of the pipe.

The conditions at the ends $x = 0$, $x = 1$ with reference to section 2.6 and Fig. (3.1b) may be directly written as,

$$X_L(0) = 0, \quad X_R(1) = 0 \qquad \ldots(2.64a)$$

$$Y_L(0) = 0, \quad Y_R(1) = 0 \qquad \ldots(2.64b)$$

$$X_L'''(0) = -M_A^x \quad , \quad X_R'''(1) = -M_B^x \qquad \ldots(2.65a)$$

$$Y_L'''(0) = -M_A^y \quad , \quad Y_R'''(1) = -M_B^y \qquad \ldots(2.65b)$$

The governing equations that apply to the left and right half of the pipe element are respectively (see equation (2.08a,b)).

$$\frac{d^4X_q}{dx^4} + u_o^2\left(1 - \delta + \frac{\delta^2}{2}\right)\frac{d^2X_q}{dx^4} - \frac{1}{4}\Omega^2 X_q - \frac{\gamma u_o \delta \Omega}{2}\left[(1-x)\frac{d^2Y_q}{dx^2} - \left(1 - \frac{2}{\delta}\right)\frac{dY_q}{dx}\right] = 0 \qquad \ldots(2.66a)$$

$$\frac{d^4Y_q}{dx^4} + u_o^2\left(1+\delta+\frac{\delta^2}{2}\right)\frac{d^2Y_q}{dx^2} - \frac{1}{4}\Omega^2 X_q - \frac{\gamma u_o \delta \Omega}{2}\left[(1-x)\frac{d^2X_q}{dx^2} - \left(1 + \frac{2}{\delta}\right)\frac{dX_q}{dy}\right] = 0 \qquad \ldots(2.66b)$$

where the subscript $q \equiv L$ with $0 \leq x \leq 1/2$

$\equiv R$ with $1/2 \leq x \leq 1$.

Equation (2.66a) and (2.66b) are four, fourth order coupled differential equations and together with the sixteen constraints given by equations (2.58a,b,c,d,e,f; 2.63; 2.64a,b; 2.65a,b) form a determinate system of equations for the four unknowns X_L, Y_L, X_R, Y_R.

The above system of equations may be solved by expressing each unknown as a truncated power series. The receptances are obtained in the same manner as outlined in section 2.6.

3.3 Results and Discussions

3.3.1 Computations Performed

Using the analyses presented in the previous sections, numerical results, listed below have been obtained. As in chapter II, the instability regions are presented as plots of non-dimensional frequency Ω versus the excitation parameter δ. All results pertain to the following pipe parameters :
$u_o = 0.6\,\pi$, $N = 2$, $\gamma = 0.8$.

(1) Determination of instability regions with $r_a = 0.2$, $\sigma_a^2 = 1$ and damping factors $\zeta_a = 0.01,\ 0.05,\ 0.1$.

(2) Instability regions are obtained to study the effect of changing the tuning ratio ($\sigma_a^2 = 0.8,\ 1,\ 1.2$) of a lightly damped absorber ($\zeta_a = 0.01$, $r_a = 0.2$).

Results presented in chapter II are used as a check, for the case: $r_a = 0$, in the absorber formulation.

3.3.2 Discussions

Convergence in the receptance values in frequency range of interest was obtained by truncating each powers series of X_L, Y_L, X_R, Y_R after 16 terms.

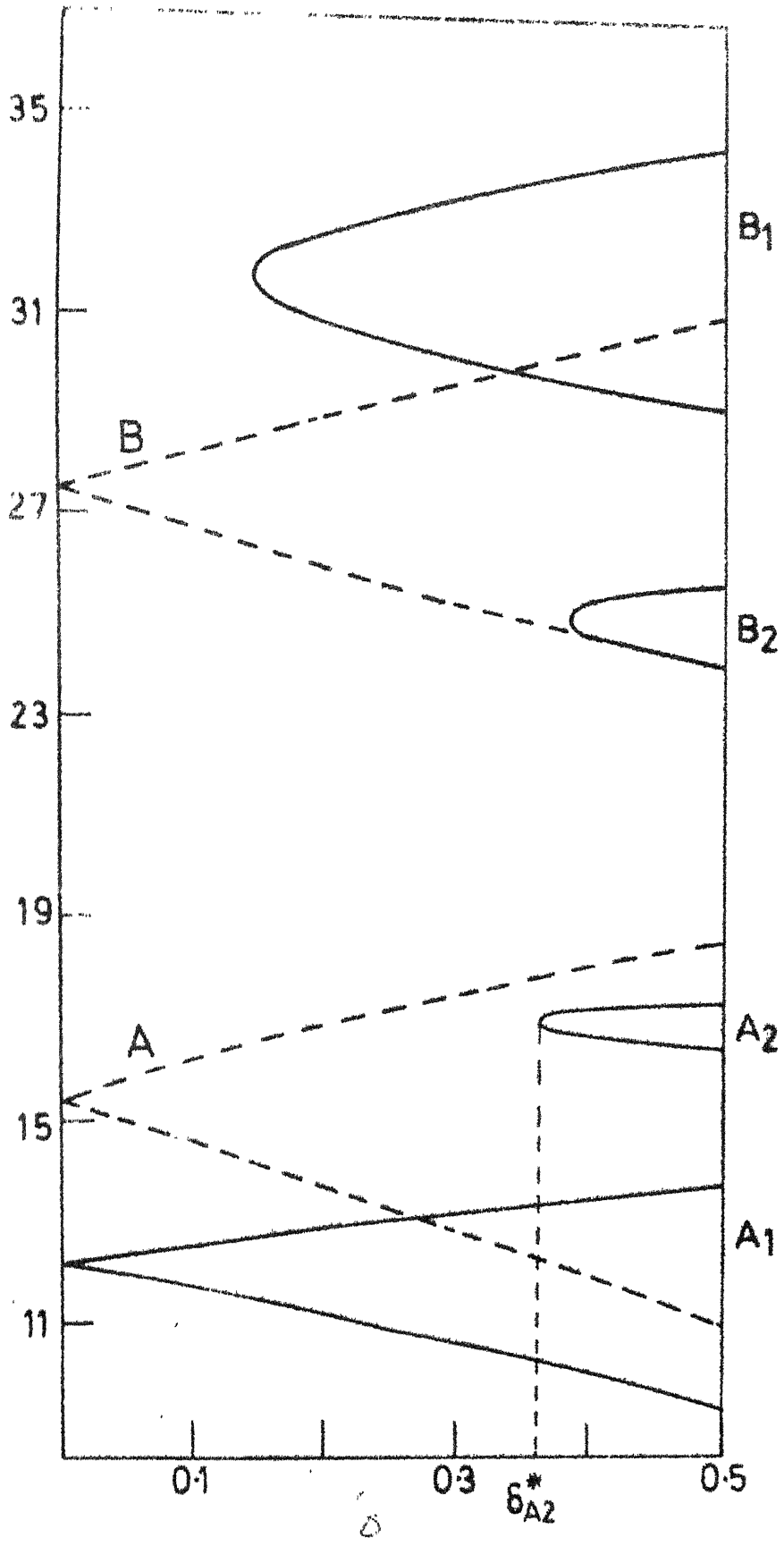

Fig 3·2 Regions principal primary instability
- - - - without absorber $u_0 = 0{\cdot}6\,\pi$, $N = 2$, $\gamma = 0{\cdot}8$,
——— with absorber $\Gamma_a = 0{\cdot}2$, $\sigma_a^2 = 1{\cdot}0$, $\varepsilon_a = 0{\cdot}01$
$u_0 = 0{\cdot}6\,\pi$, $N = 2$, $\gamma = 0{\cdot}8$

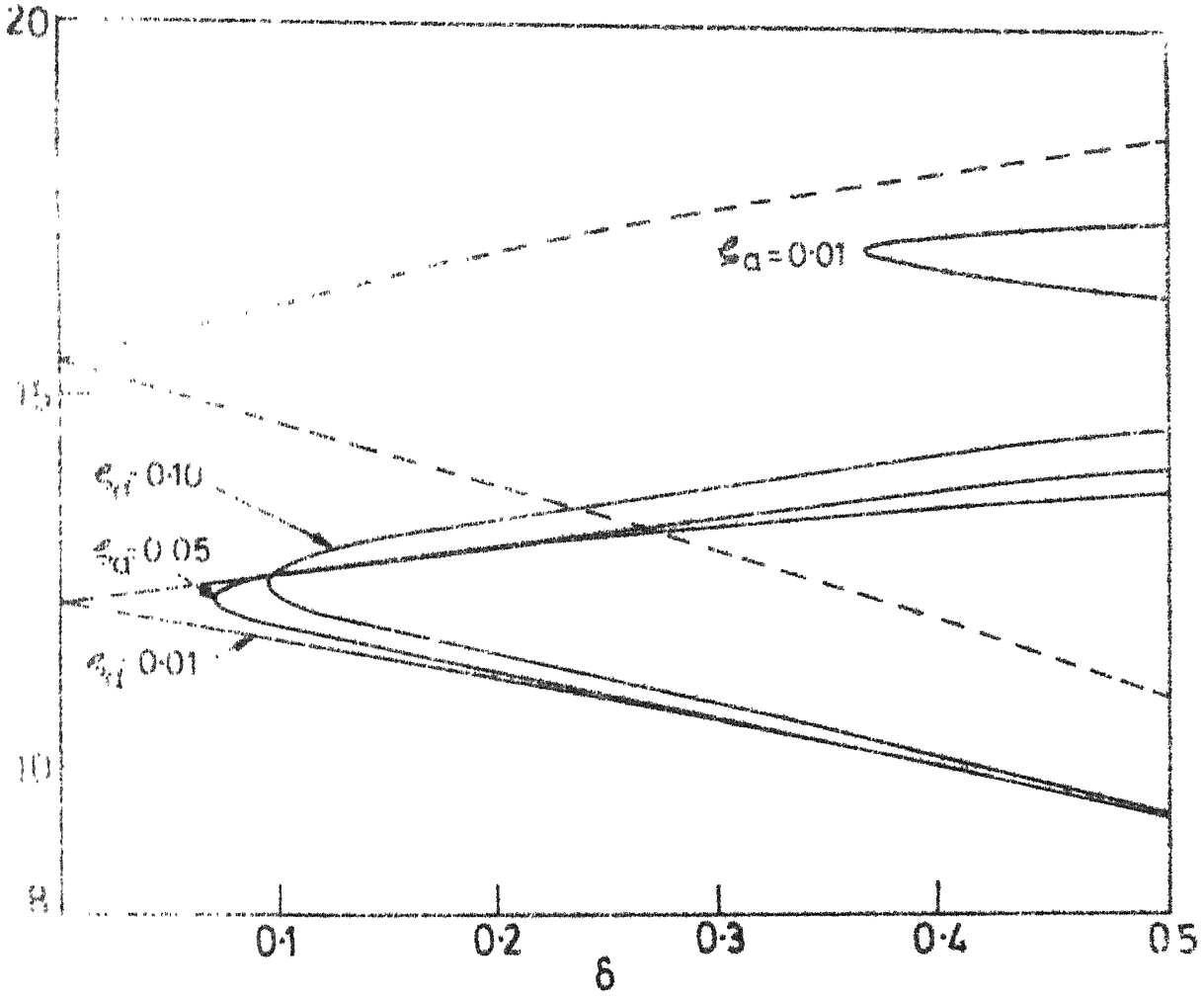

Fig. 3·3 Effect of damping factor on the first pair of principal primary instability zones (absorber case)

——— with absorber $u_0=0{\cdot}6\pi$, N=2, $\gamma=0{\cdot}8$
$\Gamma_a=0{\cdot}2$, $\sigma_a^2=1{\cdot}0$, $\varepsilon_a=0{\cdot}01, 0{\cdot}05, 0{\cdot}1$

– – – without absorber $u_0=0{\cdot}6\pi$, N=2, $\gamma=0{\cdot}8$

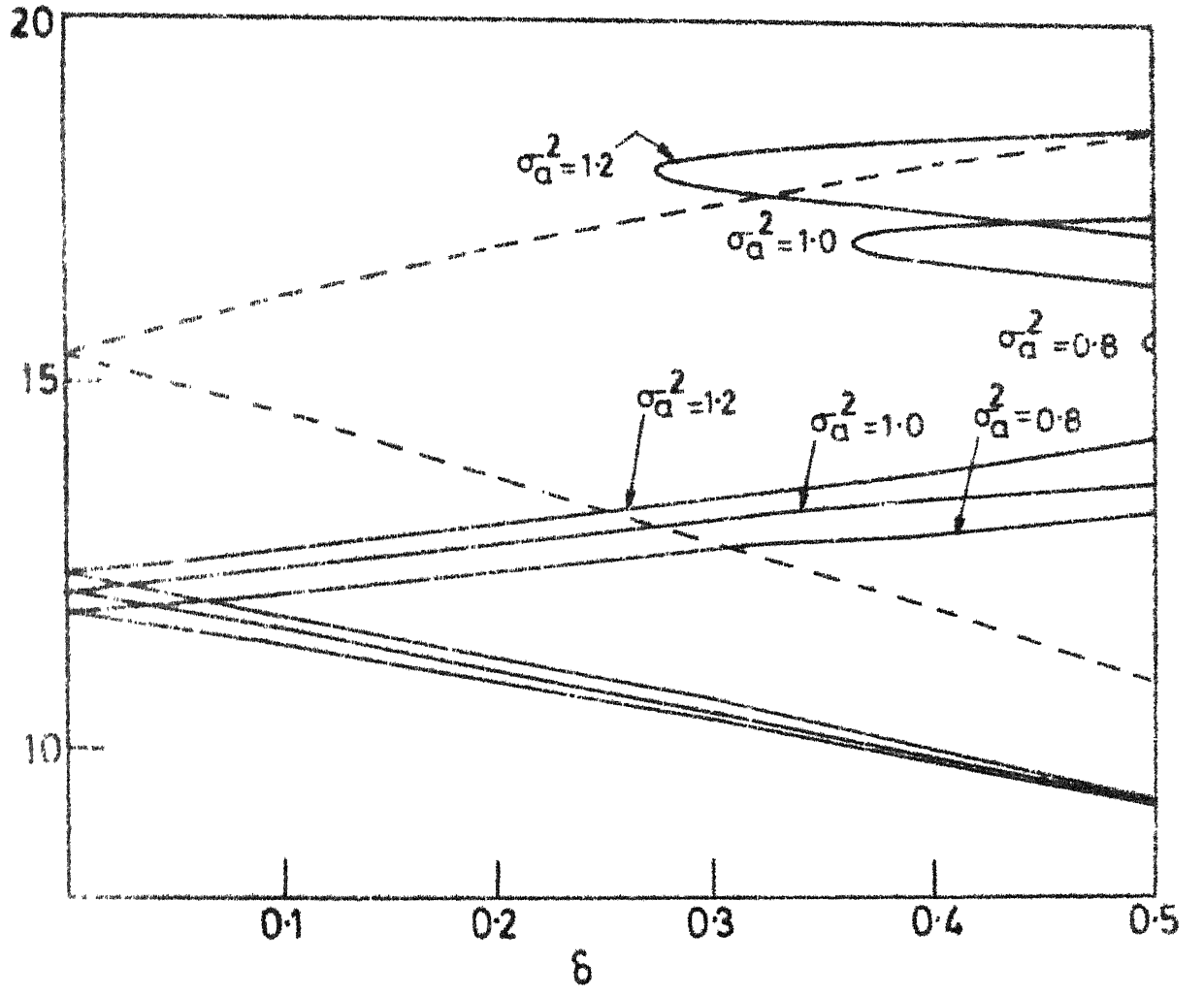

Fig. 3·4 Effect of tuning ratio on the first pair of principal primary instability zones (absorber case)

—— with absorber u_0=0·6 π, N=2 , γ=0·8

Γ_a =0·2 ζ_a=0·01 , σ_a^2=0·8, 1·0, 1·2

----- without absorber u_0=0·6 π , N=2 , γ=0·8

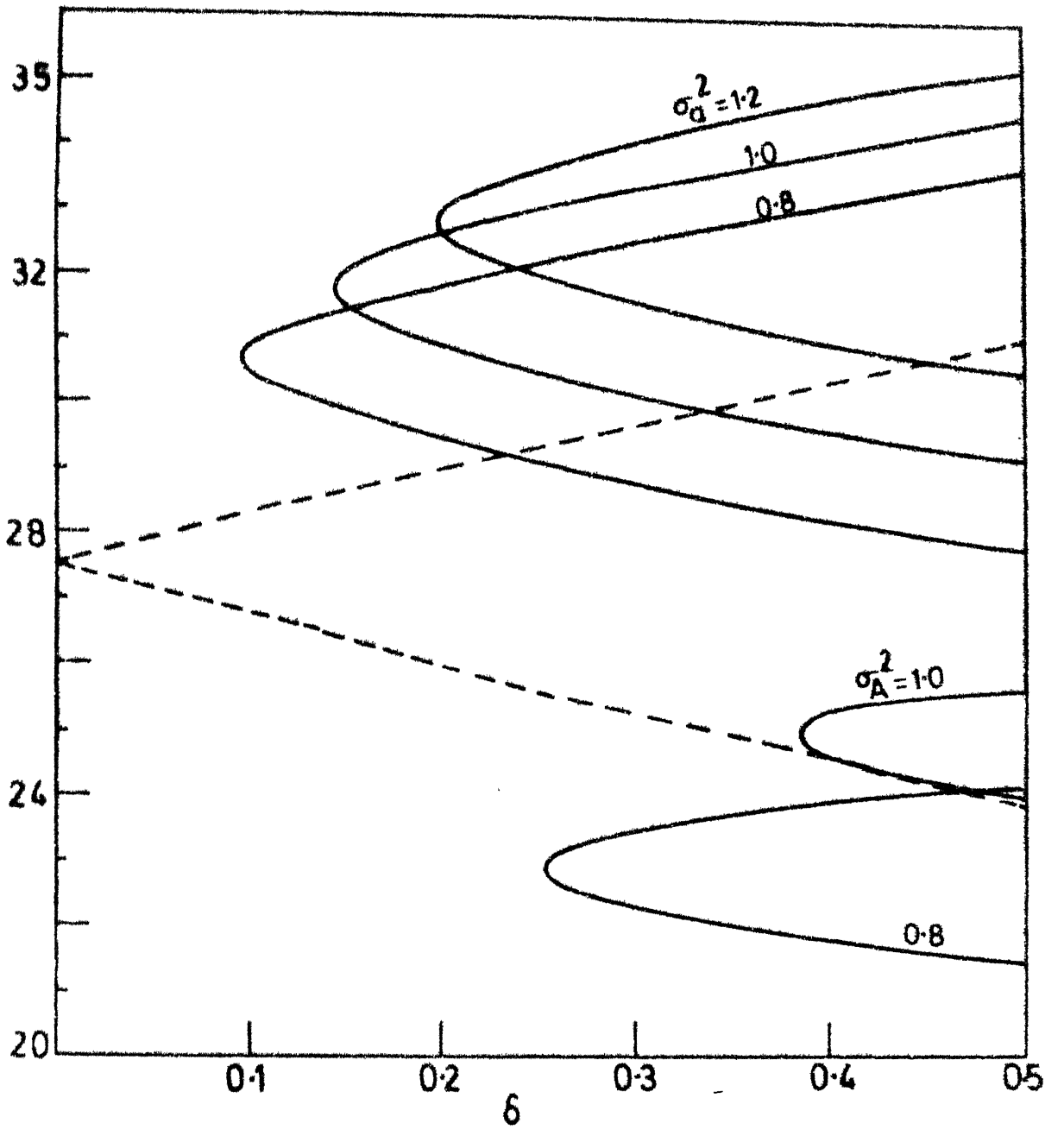

Fig 3·5 Effect of tuning ratio on second pair of principal primary instability zones (absorber case)

—— with absorber $u_0 = 0{\cdot}6\pi$, $N = 2$, $\gamma = 0{\cdot}8$
$\Gamma_a = 0{\cdot}2$, $\zeta_a = 0{\cdot}01$, $\sigma_a^2 = 0{\cdot}8, 1{\cdot}0, 1{\cdot}2$

– – – without absorber $u_0 = 0{\cdot}6\pi$, $N = 2$, $\gamma = 0{\cdot}8$

Fig. (3.2) is a plot of the instability zones for $N = 2$, $u_o = 0.6\,\pi$, $\gamma = 0.8$ and $r_a = 0.2$, $\sigma_a^2 = 1.0$ and $\zeta_a = 0.01$. In the same figure for comparison the instability zones for the same primary system parameters, without the absorber are also shown.

We observe that each instability zone (in the non-absorber case) splits into two, so that for a two span pipe we have four instability zones in the region of investigation. These zones are referred to as A_1, A_2, B_2, B_1 for convenience, as shown in Fig. (3.3). These zones are narrower in width in comparison to the instability zone without the absorber (marked A and B in the same figure). It is noted that A_2 and B_2 are narrower compared to A_1 and B_1. The zones A_1, B_1 are further apart on the frequency axis in comparison to A and B.

Besides the repositioning of the instability zones along the frequency axis on addition of a lightly damped absorber it is observed that the zones A_2, B_2, B_1 got shifted along the δ axis too. This is ascribed to the effect of damping(present in the absorber)[16]. Thus with each instability zone there is an associated critical excitation parameter δ^* (e.g. $\delta^*_{A_2}$ with A_2) such that the loss of dynamic stability (on account of a particular zone) occurs only when $\delta > \delta^*$.

At $\zeta_a = 0.01$ (which is a case of low damping) we observe that $\delta^*_{A_1} = 0$. In the range of parameters investigated it appears that generally

$$\delta^{*}_{A_2} > \delta^{*}_{A_1},$$

$$\delta^{*}_{B_2} > \delta^{*}_{B_1},$$

and $$\delta^{*}_{B_1} > \delta^{*}_{A_1}.$$

It is seen that, higher modes are significantly shifted along the δ axis. To observe the effect of damping (particularly for zone A_1) ζ_a is increased to 0.05 and 0.1. It is seen that on changing ζ_a from 0.1 to 0.05, the instability zones A_2, B_1, B_2 are swept off to the right along the δ axis so that $(\delta^{*}_{A_2}, \delta^{*}_{B_2}, \delta^{*}_{B_1}) > 0.8$. Figure (3.3) is a plot of the I mode instability zones for various values of ζ_a. From this figure we observe that zone A_1 can also be successfully controlled such that $\delta^{*}_{A_1} > 0$. The instability zone A_1 is a relatively 'hard zone' and is affected to a lesser extent by the absorber damping. Thus the qualitative effect of increased damping is to shift the zones towards the right and this effect is more pronounced for higher modes of instability. At this stage it is remarked, that the critical excitation parameter δ^{*}, is also a function of the other absorber parameters and in general, changes on varying r_a and σ_a^2 as well. The effect of tuning ratio, σ_a^2 on the instability zones is shown in Fig. (3.4) and (3.5). These plots correspond to the first and second pair of modes respectively with $r_a = 0.2$, $\zeta_a = 0.01$, $\sigma_a^2 = 0.8$, 1.0 and 1.2. For these values of parameters the effect of

changing σ_a^2 on zone A_1 is negligible compared to that on A_2. On increasing σ_a^2, A_2 is observed to shift to higher frequency and that $\delta^*_{A_2}$ also increases. The effect of changing σ_a^2 is opposite on B_1 and B_2(Fig.3.5)). On increasing σ_a^2 from 0.8 to 1.2, zones B_1 and B_2 shift to lower frequency and $\delta^*_{B_1}$ and $\delta^*_{B_2}$ decrease in magnitude. This suggests that with ζ_a fixed there exists an optimum value so that both $\delta^*_{A_i}$ and $\delta^*_{B_i}$, $i = 1,2$ are a maximum.

The effect of change in the absorber parameters is thus seen to significantly alter that instability zones, albeit in a complex manner. It may be concluded from these investigations that the effect of damping is more pronounced for instabilities in the higher modes. The optimisation of tuning ratio may be necessary in the range of parameters where σ_a^2 affects A_1 and B_1 significantly.

In actual conditions, the fluctuations in the flow are not harmonic. They may be described as a band limited stochastic process. Once the power spectral density of the fluctuations is obtained we can define the region of intersst in $\Omega - \delta$ space that is to be made entirely stable. By prescribin a suitable objective function, for e.g., (i) maximize δ^*, (ii) minimize width of instability regions, (iii) maximize frequency separation of instability zones, etc., we can suitably optimize the absorber parameters for best results.

CHAPTER - IV

CONCLUSIONS

4.1 Conclusions

From the results presented in Chapter 2 and 3 the following conclusions are drawn.

The parametric instabilities of a periodically supported pipe conveying a pulsatile flow can be conveniently analysed by the propagation constants approach. This is mentioned particularly, in view of the appearance of the space dependent term and the flow direction dependent terms which destroy the directional equivalence in the governing equation.

The coupling effect of the fluid mass ratio parameter has been incorporated in the analysis in a systematic fashion (by introducing cross receptances) and the hitherto unknown effects have been discussed. The propagation constants have been shown to be sensitive to the fluid mass ratio and it is shown that for high values of this parameter the coupling effect must be retained at all stages of analysis. For low degree of coupling it is shown that this approach is identical to the graphical approach available in the literature. The effect of increasing the fluid mass ratio is seen to broaden the instability zonesand that this effect is more pronounced for higher values of excitation parameters.

It is seen, that irrespective of the degree of coupling, the frequency pair bounding the first zone of instability corresponds to the start of the propagation bands for the respective propagation constants. The frequencies bounding the higher zones of instability do not bear a simple correlation with the plot of the propagation constants versus the non-dimensional frequency Ω (especially for the case of high fluid mass ratio). For a low degree of coupling, however, the graphical technique may usefully be applied.

The instability zones are markedly affected by the attachment of dynamic absorbers at the mid-point of each span. The methodology in the analysis is unchanged on addition of absorbers to the system, if the periodicity is retained. In the same range of frequency, the number of instability regions with absorbers are more, than those without it. However, the width of these regions are much smaller than the original regions and they can be controlled by varying the absorber parameters. With a fixed absorber mass ratio parameter, the first zone of instability is affected to a lesser extent by the change of the tuning ratio and the damping factor. The critical excitation parameter, in general, increases with higher values of the damping factor. The trend of the effects of the tuning ratio, on the different zones of instability, suggests the existence of an optimum value. Hence depending upon specific requirements, the optimum values of these parameters can be determined. Due to the breakdown of

directional parity in the system (on account of flow) the best location for the absorber needs to be ascertained in a systematic way.

The method developed in this work can readily be extended for determining the secondary and higher order ($K = 2,3,...$) instability regions as well. Moreover, unlike the Ritz-Galerkin procedure [7] the primary instability regions associated with all the modes are obtained simultaneously.

4.2 Recommendations for Future Work

In view of the simplifications and the results obtained in the present thesis, the following directions are suggested for further research.

i) Incorporation of the effect of gravity, pressurisation, axial tension and contraction which have not been explored in the present work can be undertaken.

ii) Parametric regions (with pulsatile flow) that trigger combinational resonances can be investigated.

iii) Optimisation techniques for absorber location and absorber parameters for control of instability zones can be investigated.

iv) The problem of parametric instabilities of pipes with random fluctuations in the fluid velocity can be studied.

REFERENCES

1. Ashley, H. and Haviland, G. 1950 Journal of Applied Mechanics 17, 229-232. Bending vibrations of a pipeline containing flowing fluid.
2. Long, R.H.Jr. 1955 Journal of Applied Mechanics 22, 65-68. Experimental and theoretical study of transverse vibration of a tube containing flowing fluid.
3. Housner, G.W. 1952 Journal of Applied Mechanics 19, 205-208. Bending vibrations of a pipeline containing flowing fluid.
4. Gregory, R.W. and Païdoussis, M.P. 1966 Proceedings of the Royal Society (London) A, 293, 512-542. Unstable oscillation of tubular cantilevers conveying fluid. I : Theory, 512-527; II : Experiments, 528-542.
5. Singh, K. 1977 Ph.D. Thesis, I.I.T. Kanpur. Dynamics of a periodically supported pipe conveying fluid.
6. Chen, S.S. 1971 Journal of the Engg. Mechanics Division, Proceedings of the American Society of Civil Engineers 97, 1469-1485. Dynamic stability of a tube conveying fluid.
7. Païdoussis, M.P. and Issid, N.T. 1974 Journal of Sound and Vibration 33, 267-294. Dynamic stability of pipes conveying fluid.
8. Brillouin, L. 1946 Wave Propagation in Periodic Structures. New York : Dover Publications.

9. Mead, D.J. 1971 Journal of Sound and Vibration 11, 181-187. Free wave propagation in periodically supported, infinite beams.

10. Sengupta, G. 1970 Journal of Sound and Vibration 13, 89-101. Natural flexural waves and the normal modes of periodically supported beams and plates.

11. Singh, K. and Mallik, A.K. 1977 Journal of Sound and Vibration 54(1), 55-56. Wave propagation and vibration response of a periodically supported pipe conveying fluid.

12. Singh, K. and Mallik, A.K. 1979 Journal of Sound and Vibration 62(3), 379-397. Parametric instabilities of a periodically supported pipe conveying fluid.

13. Singh, K. and Mallik, A.K. 1978 Journal of Applied Mechanics, Transactions of the American Society of Mechanical Engineers 45, 949-951. Use of dynamic absorbers to control parametric instabilities of a pipe.

14. Mallik, A.K. and Narayanan, S. 1980 Control of parametric instabilities of a periodically supported pipe with dynamic absorbers, 661-676, International Conference on recent advances in structural dynamics, Univ. of Southampton, Recent Advances in Structural Dynamics Vol.2 edited by M. Petyt.

15. Stein, R.A. and Torbiner, M.W. 1970 Journal of Applied Mechanics 92, 906-916. Vibration of pipe carrying flowing fluid.

16. Bolotin, V.V. 1964 The Dynamic Stability of Elastic Systems, San Francisco : Holden Day Inc.